Time Domain Characteristics of Human Force Control in Rejection of Transient Disturbances During Movement

by

Erin Maneri

Submitted to the Department of Electrical Engineering and Computer Science
in partial fulfillment of the requirements for the degree of

Master of Science in Electrical Engineering and Computer Science
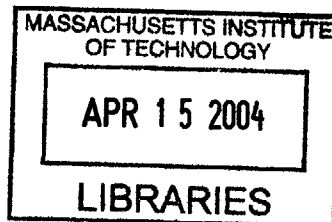
at the

MASSACHUSETTS INSTITUTE OF TECHNOLOGY

[February 2004]

September 2003

Author . . . .
Department of Electrical Engineering and Computer Science
September 5, 2003

Certified by . . .

Steve G. Massaquoi
Assistant Professor of Electrical Engineering
Thesis Supervisor

Accepted by . . . .
Arthur C. Smith
Chairman, Department Committee on Graduate Students

Time Domain Characteristics of Human Force Control in Rejection of Transient Disturbances During Movement

by

Erin Maneri

Abstract

Many tasks that humans successfully complete are more naturally represented in terms of their force requirements than their state (position or velocity) requirements. Yet the literature on force and timing is relatively underrepresented. This work was an attempt to clarify whether feedforward and/or feedback force control mechanisms might be available in human motor control. Subjects were trained and tested rejecting simple square pulse disturbance forces perpendicular to concurrent reaching movements. The data was analyzed with the goals of both verifying the feasibility of a proposed control model, and then clarifying the capabilities, limitations and properties of such a controller.

Contents

List of Figures

List of Tables

Chapter 1

Background & Problem Statement

1.1 Purpose of investigation

Researchers have combined the tools of mathematical modeling and control systems analysis with the hypotheses and established facts of neuroscience in order to contribute to the understanding of human motor control. Their findings are applied towards furthering robotic capabilites and the capabilities of those who suffer from motor disorders. While motion trajectory contol has been more extensively studied in relation to human motor control, it is not the only potentially important control mode. Especially in relation to disturbance rejection, explicit force control would in principle also be possible. Moreover, many motor control tasks might benefit from a combination of explicit force and motion state control. Humans and other animals appear to be able to shift between and possibly integrate the two control modes with particular ease. For the reasons mentioned above, it would therefore be of interest to understand how the human nervous system controls forces in relation to motion.

During motion humans frequently encounter disturbing influences. Building upon studies of motion trajectory control, two possiblities arise for disturbance rejection; one, that the same feedforward and/or feedback state dependent systems used in motion control are also used for disturbance rejection, and two, that disturbance rejection employs the explicit feedforward force control system assumed to exist for force application to the environment when little or no motion ensues. Conditt et al [3] have shown that disturbances can be rejected according to state dependent systems. However, the two modes may not be mutually exclusive. It remains to be shown whether explicit force control is available for use in rejecting transient disturbances during motion.

1.2 Physiological control of forces

As force control builds upon findings from various other subfields of motor control, the applicable background will be introduced here, along with the issues, controversies and questions surrounding motor control with particular attention to transient disturbance rejection.

1.2.1 Physiological systems involved in force generation

Locations of planning, command formulation feedback and processing consistent with state control will be introduced with the model in the Engineering Model section (2.1).

Ashe [1] compiled a comprehensive view of the role of the motor cortex in encoding static and dynamic forces. These motor cortical signals travel through the spinal cord to the limb. We expect that signals derived from motion state-based control mechanisms and those from force control are processed in the same manner by the muscles. Therefore we look to higher level control to study the nature of the signals and their waveform over time. Force controlled signals may be freeform with no underlying structure, or they may have similar structure to state controlled signals. In the case of the latter we might propose that commanded forces, analogous to submovement theories, are a combination of subforce primitives. Such primitive components are scaled in magnitude, delayed some amount after the onset of the previous primitive, then summed together for assembly of an entire command. Primitives are addressed later in section 1.2.3 while the physiological needs to generate them are discussed here.

Numerous authors have focussed on formulating hypotheses on the existence, location and properties of a neural clock employed in motor control. While many agree that such a structure exists, researchers have only been successful at ruling out possibilities rather than finding its location. Based on earlier predictions that a motor clock would be initiated with movement onset, operate at about 10Hz and be found in the cerebellum, Keating and Thach [11] recorded cells of behaving monkeys but were unable to find any oscillator below 100Hz. In their theoretical and experimental study of motor timing, Treisman et al [19] argued that multiple clocks (one for each effector) are used in motor tasks. They proposed a neurologically feasible model for these such that the frequency could be adjusted and the circuit be self-exciting.

1.2.2 Characteristics of forces generated

In a study aimed at determining limiting behavior in ballistic tasks (those that are preprogrammed, open-loop, and finish before sensory or feedback information can be incorporated), Freund and Büdingen [7] concluded that it is the neural programming, not mechanics of the system, that regulate maximum muscle contraction speed. This study looked at muscles with different force level capabilities, yet each had the same rise time to target level. In Fig. 1-1 the trajectories marked
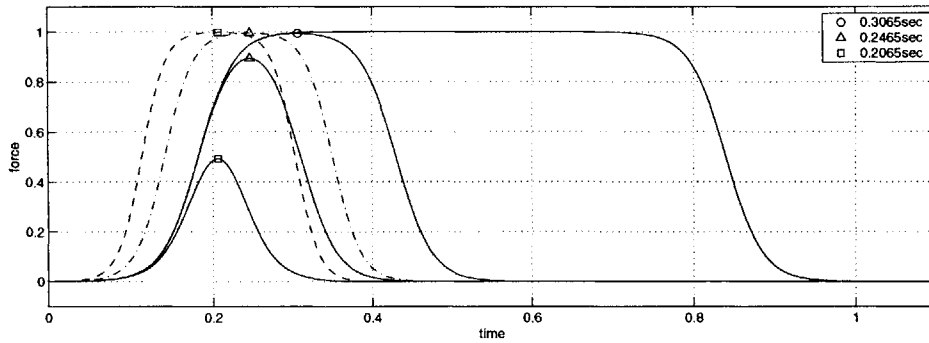
Figure 1-1: Forces: solid (dashed) lines represent proposed time-based (state-based) force generation capabilities

with squares (triangles) show two different forces attained the same amount of time, about 200ms (250ms). In the Freund study, the target levels were either torque levels (isometric) or angle displacements (movements), but, again, rise time did not vary between the two tasks so that all target levels tested were achieved in approximately 90ms. The authors did not investigate the nature of the command for the isometric task so that even though the desired output was a torque level, the command may have been posed internally as a desired joint angle change. Later Ivry [10] confirmed these temporal properties of force generation, namely the invariance in minimum time to target force.

But most recently these findings were challenged by Ulrich and Wing's [20] parallel force unit model which predicts that build up time to target force depends on target force level. Here larger forces would take longer - not equal - time to generate. Solid lines in Fig. 1-1 show the force pulses generated in four different durations when the target force level is held constant. Note the constant slope of force build up and that pulses shorter than 0.6s do not achieve the target level. Although Ivry also compared minimum force generation time for both isometric and movement tasks, the discrepency in these findings may be resolved with an understanding of whether state or force control mechanisms were involved.

1.2.3 Intermittency in feedforward position (and possibly force) control

Motor control operates over a range of frequencies. At the level of consciousness, the decision to do a motor task is discrete, but feedback from sensors is continuous, albeit delayed. Milner [14] conducted a study in which subjects were instructed to make a movement where enpoint precision was the goal. Their trajectories were decomposed into prototypial submovements, though the overall velocity profiles appeared smooth. While visual feedback does introduce some of this intermittency, it does not account for all discontinuities [4]. It is hypothesized in Thoroughman and Shadmehr that

13

normal movements are constructed of discrete "primitive" components tuned to velocity [18]. They argue that the shape of the primitives plays a role in human's ability to learn external dynamics. Ulrich and Wing [20] extend the concept of position control primitives to force control by proposing a model in which the force generated is the summation of multiple force primitives of constant magnitude scaled in duration. Their study in particular is developed with brief force pulses in mind. The current submovement models will be compared with the data from this study to determine if forces are generated with analogous subforces.

1.2.4 Compensation for transient disturbances using reference and measured plant state

Shadmehr and Mussa-Ivaldi [15] simulated and experimented with reaching movements in a viscous disturbing field. Adaptation of the model involved tuning its control parameters. The reference trajectory connecting start and finish points with a straight line (and bell-shaped tangential velocity) was input to their 'robust control system' model:

$$C(\theta, \dot{\theta}, t) = \hat{I}(\theta) * \ddot{\theta}_{ref}(t) + \hat{G}(\theta, \dot{\theta}) + \hat{E}(\theta, \dot{\theta}, t) - K(\theta - \theta_{ref}(t)) - V(\dot{\theta} - \dot{\theta}_{ref}(t)) \qquad (1.1)$$

where θ ($=\theta_{actual}(t)$) is the vector of sensed joint angles and $\dot{\theta}$ ($=\dot{\theta}_{actual}(t)$) is the respective angular velocity. $\theta_{ref}(t)$ is the reference trajectory (a straight line connection start and finish points), $\dot{\theta}_{ref}(t)$ is bell-shaped tangential velocity and $\ddot{\theta}_{ref}(t)$ is the derivative of $\dot{\theta}_{ref}(t)$. C represents the forces commanded by the controller. $\hat{I}$ is the system's approximate inertia at position θ and $\hat{G}$ represents approximations of other state dependent forces (Coriolis, friction, etc.). Together $\hat{I}$ and $\hat{G}$ model the passive system. $\hat{E}$ solves the equation $E(\theta, \dot{\theta}, t) = \hat{E}(\theta, \dot{\theta}, t)$ at $\theta_{ref}(t)$ where E is the environmental dynamics, ie the disturbance. K and V are the stiffness and viscosity matrices that restore the joints to their reference values. However, this equation does not include the known closed-loop neural signal transmission delays between arm and brain which are on the order of 20ms. Inclusion of such delays in Eq. 1.1 might give rise to instability not observed in human behavior.

Still, the simulated output trajectory was highly correlated with experimental output throughout the learning process: early in training, when the disturbing field was new to subjects, characteristic hook-shaped corrective movements were present in both simulations and experimental results, even as visual feedback was not available. In addition, after learning had occurred, catch trials were run and the behavior predicted in simulations was in qualitative agreement with that of the subjects, namely, approximate mirror image trajectories to when the field was new and unexpected. The controller was considered a potentially good physiological model as it fully encompassed the gross interaction between the arm's mechanical properties and the external force field. In addition it had the benefit of computational simplicity in that the internal model, $\hat{I} + \hat{G}$, is an ideal controller for

14

the dynamic system, not the system dynamics as such.

1.2.5 Compensation for transient disturbances using feedforward "rote" control only

The Shadmehr study provided a description of the gross behavior of disturbed movements, though the proposed computations are not necessarily neurologically feasible or accurate without the inclusion of delays. "Rote learning" is an alternative mechanism to compensate for the disturbances. Conditt et al [2] defined rote learning as a feedforward mechanism that associates external forces with internally generated temporal force compensation waveforms. They liken rote learning to open loop control, though this connection need not be implicit as feedback information may be included to satisfy concurrent motor goals. The goal of the study was to desipher whether compensation for transient disturbances was done via rote learning or formulation of an internal model of the disturbance. They state that when adaptation is a result of rote learning, generalizability outside of the practiced states is possible only so long as the time sequence of the disturbance remains constant. The continued presence of aftereffects throughout all the trials of the block was evidence of a change in feedforward component of the motor command. However the effective transfer of learned dynamics to different movements encountering disturbances having the same motion state dependence, but different temporal waveform lead them to state that adaptation was the result of a model linking environmental dynamics to arm state. These study results argue against the possiblity of the *sole* use of rote learning in adaptative motor tasks.

More recently, Conditt and Mussa-Ivaldi [3] looked into the possible existence of a temporal control component for use in adaptation to disturbing forces. The rationale for their experiments was that in order to compensate for a general time dependent disturbance field, the motor control system would be expected to employ an internally time-coded force control signal. To determine if this was the case, they conducted two experiments; a test for adaptation and a test for generalization.

Experiment: Adaptation to a time dependent disturbance field

The first test addressed the ability of human subjects to adapt to a time dependent field. The task was to make reaching movements holding on to a manipulandum that added a time dependent field, $F_x = 4.5 * (1 - \cos(2\pi(3\text{Hz})t))$, $F_y = 0$ which was synchronized with movement onset. The first block of trials within this experiment were in the null field to establish baseline behavior and correct timing of the task. In a random eighth of these trials the time dependent field was unexpectedly turned on to record the initial response to the perturbing field. Subjects were then given three blocks of trials in which the force field was normally on. In a random eighth of these trials the perturbing

force was unexpectedly turned off to determine the aftereffects of adaptation. The first experiment showed that all subjects were able to adapt to the force field halfway through the first exposure block (after about 100 trials), meaning that their baseline trajectory was fully recovered. But, as adaptation does not necessarily imply the basis (state or time) of the internal representation of the disturbance, the authors conducted experiments to assess the capability for generalization.

Experiment: Test for generalization

The second experiment included two blocks of trials which varied in trained movement. In the first block, subjects were tested making circles in either the null or time dependent fields after being trained to make reaching movements in the time dependent field. The authors note that the positions and magnitude and direction of velocities encountered in the circular movement were the same as those trained in the eight directions of the reaching movements, just in different temporal order. Because this test remained within the practiced state space, the *transferred* adaptation and *transferred* aftereffects were made evident (transferred because the required tasks in training and testing are different). In the second block of the generalization test, again subjects were tested making circular movements in either the null or time dependent fields, but this time the training demanded circular movements in the time dependent field. The data collected during this block made evident *direct* adaptation and *direct* aftereffects (direct because the required tasks in training and testing are the same). Both qualitative and quantitative comparisons were made between the adaptation trials. Because the statistically significant difference between the circular trajectories made in the time dependent field after training making circles and training making reaches in the same time dependent field, the authors had shown that even though the two training regimens required adaptation to the same field, the subjects did not build the same internal models to counteract the time dependent field.

As an explicitly time dependent mechanism was ruled out as the basis of the subject's internal representation, the authors sought to determine what the basis was. A third experiment comprised of two blocks was conducted. The two blocks differed in the trained disturbance field. Following adaptation of reaching movements to a time dependent field (first block), subjects were tested making circular movements in a velocity dependent field. The velocity dependent field, $F_x = 13 * (|\dot{x}| + |\dot{y}| - (\sqrt{2} - 2)\sqrt{|\dot{x}||\dot{y}|})$, $F_y = 0$, was formulated such that adaptation during training to this field would be completely effective against the time dependent field of the two previous experiments. In other words, for the states and velocities visited in the tasks of this study, the two fields were essentially the same. Before adaptation occurred the field the subjects felt differed only by a scaling in magnitude of less than 1.5 times, and after adaptation their percievable difference was negligible. In the second block of trials, all subjects were trained to make reaching movements in the velocity

dependent field. They were then tested making circular movements in either the velocity dependent field or the null field. This time statistical tests for similarity showed that test performance making circles in the velocity field was independent of whether training occured doing reaches in the time or velocity field, namely, the tranferred adaptation showed that subjects percieved the time and velocity dependent fields to be the same. In addition, when performance making circles in the null field was compared, the transferred aftereffects from trained reaches in the time and velocity fields showed no significant difference. From this the authors were able to conclude that a bias exists such that when subjected to a field that could be formulated as either a time or state based, the state based representation was chosen.

1.2.6 Isometric force control

That the command or control of force might be fundamentally different for isometric or movement tasks was proposed in Tax et al [17]. The difference in control can be observed as motor units that operate at correspondingly different firing frequency or recruitment levels independent of the net torque generated. Subjects in this study were asked to make movements in the presence of both constant and increasing, assistive or counteractive forces. In some trials subjects were asked to generate forces as movements were externally imposed. Upon confirmation of differing control signals the authors went on to determine the neural basis for the difference.

1.3 Time-based force control rejection of disturbances reconsidered

As few solid conclusions have been reached so far in the theory of human force control, further concepts remain to be hypothesized and tested. Considering the possibility of the same maximal rate of specifying torque and position targets noted by Ivry [10] and attempting to use a very simple, nearly symmetric model, it is proposed that control of movement and force are analogous but, in principle, independent. Previous studies have shown that like position control, force control utilizes feedback signals [16]. We then assume that the feedforward components of both position and force control systems are explicitly time-dependent waveforms, $x_{ref}(t)$ and $F_{ref}(t)$. Each or both of these can be adapted under appropriate conditions. Moreover, the weighting of position control versus force control systems may be adjustible according to task demands. The position control system appears to make use of proportional, derivative and integral processing [13] to generate *implicitly* the forces needed for motion control. For the moment, we propose that the force control system has no further signal processing (other than force feedback) and thereby controls force *explicitly* in a time-dependent manner. Compliant control used in robotic manipulators is a generally similar

concept.

1.3.1 Where things stand

The second Conditt paper [3] failed to rule out the possibility that feedforward, time based mechanisms were being used for disturbance rejection. In fact, they leave this option open in mentioning that state based feedback mechanisms are the *preferred*, not only, mechanism available. It is conceivable that the experimental setup inadvertently biased the outcomes as desiphering between the time and velocity dependent disturbance fields was anywhere from difficult to impossible. Although subjects appear to have been employing state based feedback mechanisms regardless of the basis of the disturbance, it is proposed here that further testing might show that the feedforward mechanisms believed to be applied in isometric tasks can also be applied in disturbance rejection.

Ulrich and Wing [20] argue for subforce primitives when the goal is to create brief force pulses. Their discussion includes no compelling reason as to why this concept might not be extended to other circumstances, in particular to disturbance rejection.

1.3.2 Hypotheses for force pulse rejection of disturbances

This project aims to combine these two remaining issues from the Conditt and Ulrich studies. The earlier discussion was an attempt to point out the similarities in position and force control and the similarities in motion and disturbance rejection. In the situations where conclusions or hypotheses exist for one type of task or control scheme, it makes sense to test whether the same holds in the other. Carefully planned training and testing procedures may illuminate the relative contributions of position and force control mechanisms.

If it turns out that force control is indeed used in disturbance rejection, then we hypothesize that it can operate independent of state, but that the minimum duration of force pulses generated under force control mechanisms are *longer* than the minimum force pulse durations generated under state based control. This is because we expect that all explicitly commanded signals have a minimum duration of 90-100ms. Therefore signals of shorter duration must be calculated implicitly. Freund and Büdingen [7] showed that minimum force pulse times are on the range of 90ms, which would indicate that these were computed explicitly, as a force command. Milner [14] found submovement durations as short as 100ms assumed to have been controlled with state based mechanisms. In the case of 100ms submovements, the implicit forces calculated in the cerebellum are some linear scaling of the second derivative of position, namely force pulses that occur at two times the frequency of the minimum movement time, or 50ms. According to this hypothesis, Ivry's subjects would have had state based intent and been represented by the dashed lines in Fig. 1-1 whereas Ulrich's subjects would have been working in the time basis and been represented as the solid lines.

Confirmation of the use of force control in disturbance rejection would add to the list another mechanism to consider in motor control studies. Apparent discrepencies in limiting behavior might be reconciled as explained above. It would remain to be shown what type of neural mechanisms are employed, though, again, if the characteristics of the control schemes are similar, one might first look for similar neural mechanisms.

1.4 Problem statement

This investigation attempts to determine whether subjects can employ something other than motion state-based control for successful disturbance rejection. It is expected that explicit time dependent force control can be used for rejecting disturbances, although at a lower frequency than if motion state-based control were used. If the data is in accordance with the expected properties of force control, a new model that treats force and position equivalently and can account for qualitative features of subject's data will be proposed. As the default method of disturbance rejection in the literature up until now has been state based, an understanding of the characteristics of force control will be used to justify the existence of such a controller. If these hypotheses can be confirmed, we might conclude that humans have more options than previously thought for dealing with the unique situation that each motor task presents.

Chapter 2

Strategy & Methods

First an engineering model of physiological time-based disturbance rejection is developed. Then experiments are run in which human subjects hold a manipulandum handle that injects programmed disturbances and records two dimensional position and three dimensional force data. The subjects are acquainted with the disturbance in an isometric rejection task and then asked to reject the same timed force disturbance while making a point to point reaching movement. Experimental results are analyzed and the model verified to capture the dynamics of human behavior.

2.1   Engineering model

We propose that motion tasks that emphasize position control are commanded with a cartesian reference trajectory x_{ref} in the cerebral cortex, Fig. 2-1. Although it is believed that this command is then reformatted and processed in joint coordinates, for the purposes of this study we will assume the cartesian workspace throughout for the reasons explained in the following paragraph. Flash and Hogan [6] demonstrated that when asked to make "natural" point-to-point movements, subjects move along an approximately straight line where the tangential hand velocity is bell shaped (minimum jerk) in cartesian coordinates. Therefore reference trajectories used in this model take such a form.

Massaquoi [13] proposed controller and two-joint plant models for simulating point-to-point arm movements in the horizontal plane. This model was simplified to a one dimension *nonr*otational problem for this study as most of the x displacement can be attributed solely to the shoulder muscles and $x \approx \theta_{shoulder} \times$ *moment arm*. This moment arm does change a moderate, predictable amount during the reaching movement, but a simplifying assumption that the moment arm is fixed is made, so $x \approx \theta_{shoulder}$.

Preliminary simulations demonstrated the functionality of the controller for the tasks in this study by matching simulated outcome to that of human subjects for time based disturbance rejection. Various disturbance rejection methods were used as will be explained in the Design section (2.2.1).
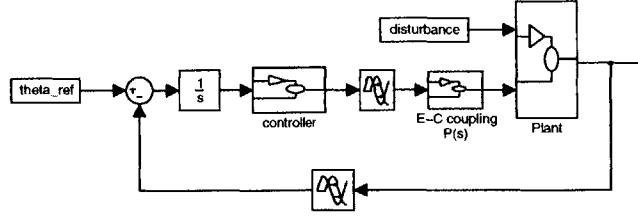
Figure 2-1: Massaquoi model
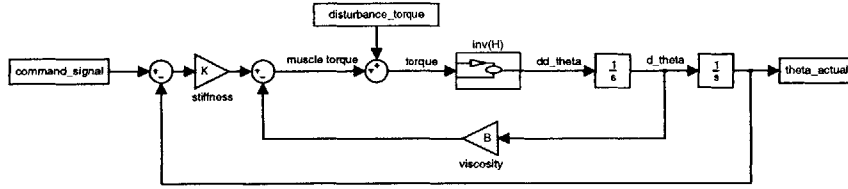
Figure 2-2: Plant

The model in Fig. 2-1 includes two uni-directional delay components for the time between signal processing in the brain, travel through the spinal cord and arrival at its effector (about 20ms each to and from arm muscles). The "activation filter", $\frac{\rho^2}{(s+\rho)^2}$ accounts for electromechnical coupling and introduces additional phase lag.

2.1.1 Musculoskeletal plant and disturbance

The arm dynamics are a function of forces generated in the muscles, $F_{muscles}$, from commands and reflex action, $U(t)$, and those applied to the arm from external sources, F_{dist}, according to Newton's second law:

$$\ddot{x} = M^{-1}(F_{muscle} + F_{dist}) \tag{2.1}$$

where

$$F_{muscle} = k(P(s)U(t) - x) - B\dot{x} \tag{2.2}$$

F_{dist} is that measured at the end effector. For our purposes the arm is modeled as a one-joint manipulator which approximates a damped mass-spring system through the damping coefficient B and stiffness coefficient, k. The mass is represented as M, again approximating a constant moment arm and one dimensional motion. The influence of gravity has been avoided by restricting movements to those in the horizontal plane. The arm model is shown in block diagram form in Fig. 2-2.

The disturbances are introduced directly into the plant. The disturbance used in experiments

21

and simulations is represented here in cartesian space by:

$$F_{programmed-x} = \begin{cases} \frac{4N}{25ms}t & \text{if } dist_{on} \le t < dist_{on} + 25ms \\ 4N & \text{if } dist_{on} + 25ms \le t < dist_{on} + dist_{dur} - 25ms \\ 4N - \frac{4N}{25ms}t & \text{if } dist_{on} + dist_{dur} - 25ms \le t < dist_{on} + dist_{dur} \\ 0 & \text{otherwise} \end{cases} \quad (2.3)$$

$F_{programmed-y}$ is zero throughout the study. $dist_{on}$ is the random onset time for the disturbance (according to the description in Sec. 2.2.2, see also Fig. 5-2).

2.1.2 PID controller

The controller is a modified PID controller (see Fig. 2-3) modeling the proposed cerebellar contribution to movement control [13]. The controller has been modified from a standard proportional-integral-derivative (PID) controller by addition of an integrated command signal that is combined with proprioceptive feedback before being sent to the arm [13]. This recurrent signal (or efference copy) helps with stability by producing phase lead in the delayed control environment. Again, this model is favored for its realistic performance, computational simplicity and correspondence with established neural anatomy.

This model contains many of the same components included in Shadmehr's model (Eq. 1.1), the important difference being that the model used in this study includes a controller designed for the *delayed* control environment. Still, the net dynamics of the system, $x_{actual}(t)$, is the solution to a differential equation which includes plant, environmental and controller dynamics [15], similar to Eq. 1.1.

2.1.3 Augmented force control

To adapt Massaquoi's model for this study, we have augmented the position feedback controller, U_{LL} with additional control signals. The spinocerebral and peripheral delays, ΔT_{sp} and ΔT_{pr} respectively, are both 10ms long. Therefore any 10ms delay will be denoted Δt in the time domain (and $e^{-sT_{sp}} = e^{-sT_{pr}} \Leftrightarrow \Delta_s$ in the Laplace domain). The augmented control signal can be denoted:

$$U(t) = U_{reflex}(t - \Delta t) + U_{LL}(t - 2\Delta t) + U_{command}(t - 2\Delta t) - ffb(t - 2\Delta t) \quad (2.4)$$

Included in this equation are a spinal reflex feedback loop, U_{reflex}, and a long loop force control servo, $U_{command}$-ffb that operates similarly to the position feedback controller, except for that this model is not routed through the cerebellum. Combining the components above, the model used in this system can be written:

22
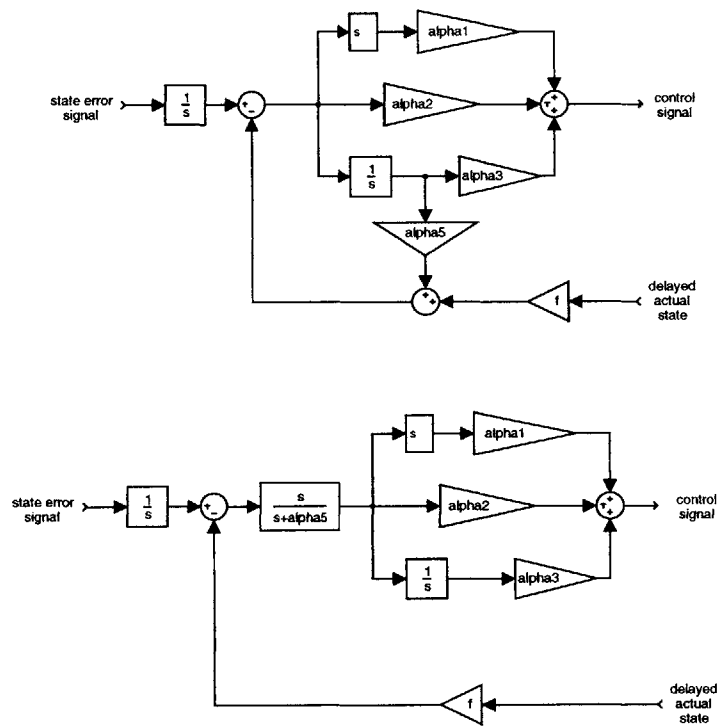
Figure 2-3: PID Controller, top shows efference copy and bottom shows the same system structured more compactly
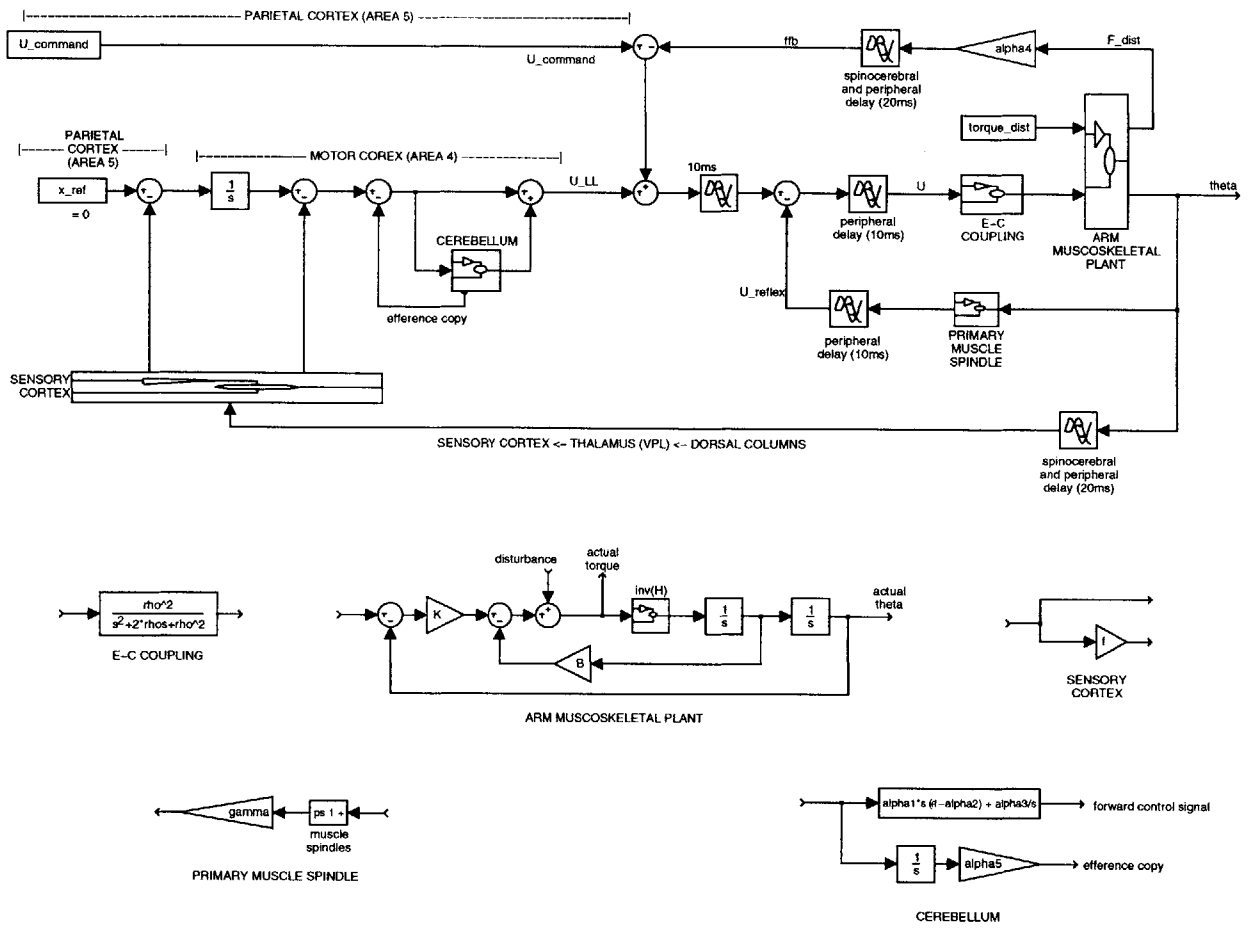
Figure 2-4: Maneri/Massaquoi model

$$P(s)U_{command}(t) = \frac{M}{K}\ddot{x}(t) + \frac{B}{K}\dot{x}(t) + x(t) - \frac{1}{K}F_{dist} - P(s)[U_{LL}(t-2\Delta t) + U_{reflex}(t-\Delta t) - ffb(t-2\Delta t)]$$

$$(2.5)$$

$$U_{reflex} = x(\Delta_s(1 + ps)\gamma(-1))$$

$$U_{LL} = x\left(\Delta_s(1 + fs)(-1)(\frac{1}{s})(\frac{\alpha_5 s}{s + \alpha_5})(\frac{\alpha_1 s^2 + \alpha_2 s + \alpha_3}{s})\Delta_s\right)$$

$$ffb = F_{dist}(\alpha_4 \Delta_s \Delta_s)$$

$$P(s) = \frac{\rho^2}{(s + \rho)^2}$$

See Fig. 2-4 for a block diagram representation and anatomic divisions. Augmenting a position control system with force control along the same spatial dimension controls stiffness. However, when force and position are controlled along orthogonal dimensions, they may be controlled independently. We will consider orthogonal force and position control as the forces studied by Conditt and Mussa-Ivaldi were perpendicular to the motion.

2.1.4   Simulation

The above model was implemented in continuous time using Matlab's control toolbox software. Mechanical and neural parameters were obtained as explained in the Data Analysis section (2.4). The disturbance applied in the simulation matches the disturbance programmed to the manipulandum (see Eq. 2.3).

2.2   Experimental tasks

Many similar experiments have been done, but purposefully combining state *and* force control components and characterizing limiting behavior of the latter are unique to this study. From the researcher's point of view it requires extreme care in design so that we may have confidence in the reasons for our findings.

As has been alluded to, previous experimental methods have not caused subjects to use an explicitly time-based system for disturbance rejection. Two possible approaches to encourage subjects to learn a time-based mechanism are training the subjects to do kinematically different movements

in the same time dependent field to reduce correlation between the field and the state, and explicitly stating that the force disturbance they will experience is time dependent. It was expected that the distinction between state and force control is the only determinant of maximum force generation speed, not whether the disturbance rejection was done while stationary or with concurrent movement.

Preliminary tests were conducted to increase the likelihood that the desired findings could be achieved as clearly and simply as possible. That humans can employ force control systems was indicated in these early tests. The following details the considerations made when designing the tasks to increase the likelihood that the desired interpretations may be made following data analysis.

2.2.1 Task design considerations

Successful disturbance rejection is demonstrated when the undisturbed trajectory is recovered in the presence of external, time-based disturbances. To design a procedure to establish whether time-based or state based compensation is being learned by the subject the following considerations were entertained. Let $\Delta U(t)$ represent the additional motor command at the plant input needed to reject the disturbance, ie from Fig. 2-2 $U(t) = -\frac{(s+\rho)^2}{\rho^2} K^{-1} F_{dist}(t)$, and Δt is the unidirectional (loop) delay.

1. Increasing the stiffness of the arm, while relatively energy consuming, can be effective at nonspecifically supressing external disturbances.

2. General state-dependent, pure feedback control: Adaptation to a particular disturbance could occur by essentially forming a look-up table which associates measured state variables with external disturbance. Here $\Delta U(t) = f(x(t - 4\Delta t), \dot{x}(t - 4\Delta t), ...)$.

3. Linear state error-dependent control: Disturbance rejection can be achieved via adaptation of cerebellar controller gains and/or forward command $x_{ref}(t)$ to generate $\Delta U(t)$ implicitly. This will produce $\Delta U(t) = f_L(\int e(t - \Delta t), e(t - \Delta t), \dot{e}(t - \Delta t)) = \alpha_3 \int e(t - \Delta t) + \alpha_2 e(t - \Delta t) + \alpha_1 \dot{e}(t - \Delta t)$ according to the model of Massaquoi [13] that is being used. Here f_L is the action of the cerebellum and cerebral cortex and $e = x_{ref}(t) - x(t - 2\Delta t)$ which is proposed to generate derivatives and integrations of the error as well.

4. Motion state reference command-dependent pure feedforward control: $\Delta U(t) = f(x_{ref}(t - \Delta t), \dot{x}_{ref}(t - \Delta t), ...)$, can be a fixed function (or look up table) of just the motion, command, reference independent of actual state feedback. This is a time dependent command but bears a fixed relation to the intended motion. When exposed to an external force the reference trajectory would be opposite in direction and appropriately scaled (from a position to a force) in magnitude.

26

5. Commanding an explicit time-based reference force signal, $U_{command}(t)$ (see Fig. 2-4) that is specified independently of $x_{ref}(t)$ for use as a feedforward component of control would also be sufficient to reject external disturbances. $\Delta U(t) = U_{command}(t - \Delta t)$. This mechanism is analogous to "rote learning" discussed earlier.

Alternatively a subject could *combine* two or more of the above methods, as did Shadmehr [15] with #2 and #4 above. But if the subject were to employ both force and state based signals the system could become overdetermined. These means of compensation have been simulated, but confirming them experimentally is the challenge proposed here. The goal is to determine whether, for appropriately designed experiments, subjects will employ a reference force signal, $U_{command}$, to adapt to external forces. To rule out the other compensation mechanisms, *limiting behavior* and *direct aftereffects* of adaptation will be determined and analyzed as follows.

1. Trials in which the expected disturbance does not occur are commonly referred to as "catch trials". "Aftereffects" are the motions or forces that are seen to occur when specifically programmed compensations are not met with an actual disturbance. Early on in exposure to a disturbance the aftereffects may have little form, but upon successful disturbance rejection by feedforward means, aftereffects are approximately equal in magnitude and opposite in direction to the deviations caused by the disturbance. If the subject compensates purely by increasing arm stiffness, aftereffects would not be seen during catch trials.

2. Because look-up tables, or learned functions, are based on previous experience with the disturbance, this method of adaptation would be insufficient for counteracting the same disturbance under novel values of the associated variable. More specifically, successful rejection on initial exposure to the same timed disturbance force that produced different motions, ie different $x(t)$ would be sufficient to show that a pure feedback look-up table is not being used.

3. If the subject adapts by adjusting cerebellar control gains and/or forward command input $x_{ref}(t)$ to provide implicit force control, then the minimum force pulse duration would not differ depending on whether motion state control or force disturbance rejection is being performed. Per the discussion in Sec. 1.3.2, if force disturbance rejection is achieved implicitly by cerebellar processing of a forward command lasting no less than 100ms (as assumed for position commands), then owing to the error signal processing by the cerebellum, force transients with rise times to maximum shorter than 50ms could be generated for force compensation. On the other hand (see #4 and #5), if cerebellar processing of a 100ms feedforward signal is not present, such a short force transient would not be expected. The maximum force speed rejection data from this study will be compared with data from other studies in which desired positional changes result in force pulses of half the duration.

4. Arguing similarly to #2 above, successful rejection of initial exposure to the same time-based disturbance force that occurs with different relationship to $x_{ref}(t)$ would be sufficient to show that a pure feedforward reference command dependent look-up table is not being used.

5. Lastly, if the subject successfully counters a time-based force disturbance that is correlated with neither $x(t)$ or $x_{ref}(t)$ when achievable using force commands that rise to peak in $\geq$100ms, and is *un*able to compensate for disturbances requiring more rapid rise to maximum time implicit cerebellar control of state is not likely. This work intends to confirm use of this method.

2.2.2 Task descriptions

Reaching movement

Preliminary experiments indicated that the best way to encourage the use of a time based force controller during movement is to minimize the correlation between force requirement and state. A reaching task was required concurrent to the perpendicular force rejection task which will be cued and occur at random times over the course of the movement. The goal is for the subject to decouple the force and state requirements, to prevent the merging of the two into a single task.

Initially, to develop automaticity, just the reaching movement is trained. The requested movement, as indicated by a moving tracking spot, is 20cm in the positive y direction lasting 3 seconds and has bell shaped velocity profile. Subjects are cued to begin each movement after two seconds of rest from the previous trial. Once the subject becomes confortable completing this task (about fourty trials), they may rest five minutes before beginning force rejection tasks.

Disturbance rejection

To establish the ablity to employ explicitly *timed* force control in disturbance rejection and the minimum duration disturbance that can be effectively rejected, subjects completed twelve trial blocks at progressively shorter disturbance durations (in Eq. 2.3 $dist_{dur}$ = 250ms, 200ms, 150ms, 125ms, 100ms and 75ms). Block A, involved isometric tasks, and block B movement tasks, as explained in detail below. Tasks occurred in the following order: A-250, B-250, A-200, B-200, A-150, B-150, etc.

- For block A, isometric force rejection, the manipulandum (see Sec. 2.3) was programmed to quickly ramp up to a target force level in the x direction, hold that force, and then ramp back down to the initial baseline force (Eq. 2.3). The subject was cued so that the duration and onset of the disturbance was apparent. Their task was to produce a force equal and opposite to the manipulandum force (in the negative x direction). Successful tasks resulted in no movement, which may be evident by the cursor on the computer display screen. The subject then rested five minutes before beginning block B.
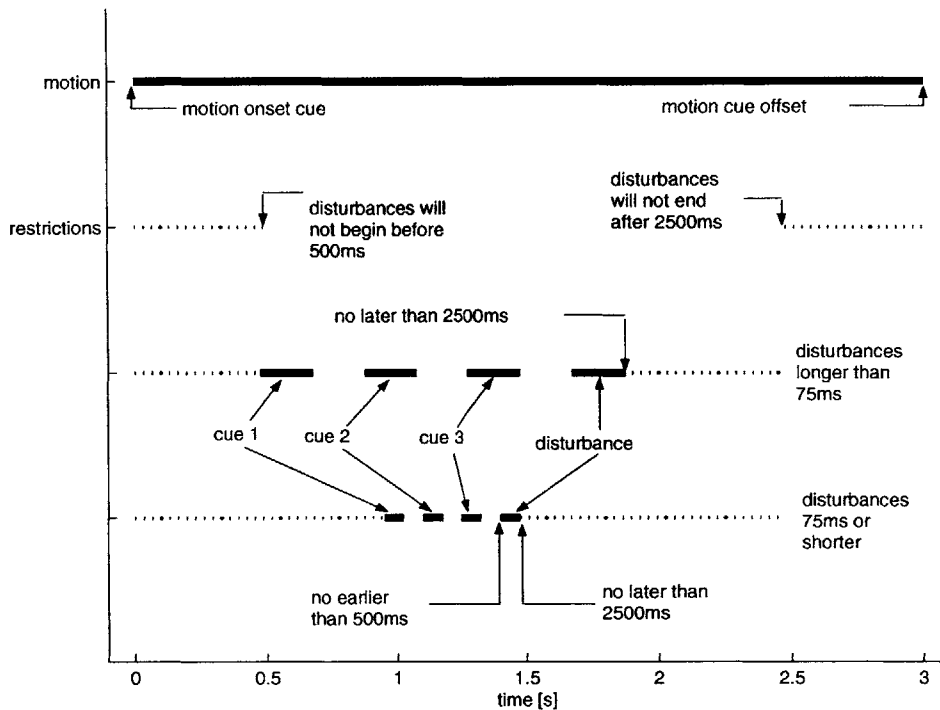
Figure 2-5: Timing of Block B trials

- Block B combined the reaching movement in the positive y direction and force rejection in the x direction. In these trials, outward reaches were cued as they were initially, and at a random time during the movement the disturbances occurred, following the same cuing scheme as in block A. Figure 2-5 is a graphical layout of the experiment timing. A random cueing sequence and hence disturbance onset time ($dist_{on}$ in Eq. 2.3) caused disturbances to occur throughout the reaching movement, minimizing the correlation of the disturbance with motion state. Subjects were instructed to maintain smoothness (bell shaped velocity trajectory) and straightness in the reaching movement while rejecting the disturbance. During the first three trials of each block B iteration, subjects were instructed to make the movement *without* trying to reject the disturbance, termed 'no resist' trials. This data gave subjects the opportunity to get a feel for the disturbance, as well as provided data from which to compute each subjects' stiffness, viscosity and inertia for use in the simulations. Catch trials, with 15% chance of occurence, were randomly inserted into the blocks as well. Subjects then rested for ten minutes before repeating blocks A and B at a faster disturbance speed.

Subjects were asked to read the instruction sheet included in the appendix and discussed the process with the investigator. They completed the tests in two sessions to avoid experimental fatigue and allow them time to become familiar with the novel requirements. In the first (training) session

29
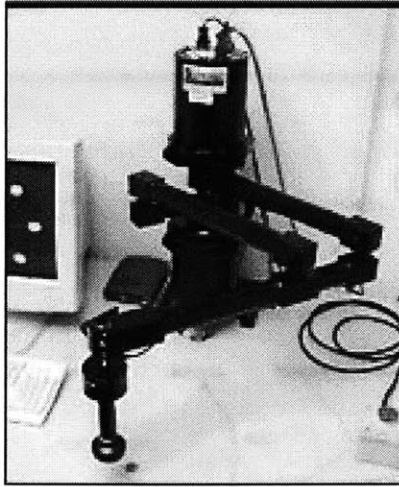
Figure 2-6: Manipulandum setup

subjects made the baseline movement 40 times, and each of the disturbance rejection tasks 60 times. When they returned 12-48 hours later the second (test) session was 20 reaching movements and 40 trials each of the twelve disturbance rejection tasks.

Preliminary experiments had indicated that the maximum speed that subjects could make forces at was the same in the isometric and moving tasks. Immediate ability to reject the disturbance with the onset of concurrent movement was expected and would demonstrate the ability to generalize. A successful trial which keeps the time and state requirements independent would show that both systems exist and can operate alone.

2.3 Data collection

Subjects and experimental setup

The goal was to collect data from two to four right handed subjects with no known neurological disorders. Subjects were seated in a straight backed chair and instructed to move only their shoulder and elbow joints.

Manipulandum and software

Current position and cueing were shown on a monitor located at eye level approximately 60cm NNW from the subject (see Fig. 2-6). Screen refresh rate was 25Hz. Subjects held on to the end of an Interactive Motion Technologies (IMT) two link manipulandum designed for both patient rehabilitation and research purposes. The manipulandum both recorded movements and introduced disturbances. The manipulandum runs under RT Linux operating system with controllers programmed in C and

the displays in TclTk. Analysis was done under the Debian Linux operating system using Matlab software.

Measurements

Position and force data were sampled at 500Hz, the variables recorded were: time t, x and y position (converted with C programs from manipulandum shoulder and elbow angles), force recorded at the force transducer on the manipulandum's handle F_{dist-x} and F_{dist-y} (converted from shoulder and elbow torques), and force onset time $dist_{on}$ (to align the random offset disturbance starts). Velocity was computed from position data using a bandlimited differentiating filter (to smooth the measurement noise) with Matlab's lsim command.

2.4 Data analysis

Qualitative (plotting) and quantitative (statistical) methods were employed in the analysis of each subject's block B (movement) tests. First, subject's data was to be checked for the characteristics that relate to the mechanism of force control (see the Design section 2.2.1). It was to be verified that the trajectories from moving catch trials showed movement opposite the direction of the expected disturbance. F_{dist-y} was checked to see that, in general, the disturbance caused neglibible y direction forces. Therefore from here F_{dist-x} will be written F_{dist}. Trial by trial analysis of each subject's force data (F_{dist}) would be done to determine the ability to employ a time based force control system as will be described below.

2.4.1 Estimation of physical parameters

The arm's stiffness and viscosity are generally considered to be functions of muscular activation level, increasing during motion. Because all the analysis would be done on block B (movement) data, the parameters were estimated using the first few movement trials at each disturbance duration. Similar to the rationale used by Gomi and Kawato [8] in determining arm mechanical impedance values, the disturbance pulses perturbed the arm and the stiffness, viscosity and mass could be determined from the damped spring-like motion that ensued afterwards (Eq. 2.5 with $U_{command} = 0$). For the purposes of analyzing the response using a one degree-of-freedom cerebellar system model, the simplifying assumption that the response in the x direction could be studied independently of y position was made. The consequences of this assumption need to be tested in future experiments. Linear least squares regression was run on the rearranged system model, Eq. 2.5 with $U_{command}=0$

for these 'no resist' trials.

$$\ddot{x}(t) = -\frac{B}{M}\dot{x}(t) - \frac{K}{M}(x(t) - P(s)[U_{reflex}(t - \Delta t) + U_{LL}(t - 2\Delta t) - ffb(t - 2\Delta t)]) - \frac{1}{M}F_{dist} \quad (2.6)$$

. The neural, parameters $(\rho,\ \alpha_1,\ \alpha_2,\ \alpha_3,\ \alpha_4,\ \alpha_5,\ f,\ p,\ \gamma)$ were tuned by trial-and-error so as to minimumize both the calculated $U_{command}$ for 'no resist' trials. After hand tuning, a constrained optimizer was applied.

In an attempt to normalize error measurements for comparison from one disturbance duration to another, squared velocity error was computed, as deviation from desired velocity would be less dependent on disturbance duration than would position. To further normalize these values, the integrated squared velocity error was divided by the velocity error for 'no resist' trials at that same disturbance duration.

2.4.2   Modeling and estimation of $U_{command}$

Analysis was done with the hopes of determining whether a force error signal, $U_{command}$-ffb was included in the control signal $U(t)$ to reject the disturbance. $P(s)U_{command}$ was calculated for the 'resist' trials. The region of the signal expected to be zero (from the beginning until at least 300ms before the disturbance) was normalized to aid in the fitting process. In general this region of data was very close to zero anyway. To determine the 300ms cutoff we studied all the data to determine the earliest legitimate force rejection efforts and these rarely began more than 300ms before the actual disturbance period. Because the single-joint model was unable to account for the multi-joint dynamics that arose about 50ms after the disturbance turned off, the prototypical pulse was not fit beyond this region. To accomodate for other idiosyncrisies not captured by the model, $U_{residual}$ (from the 'no resist' trials) was subtracted from $U_{command}$

In analogy to discrete position step changes postulated for position control, the hypothetical $U_{command}$ was modeled as a square pulse $\tilde{U}$:

$$\tilde{U}(t, t_p, \tau_p, h_p) = \begin{cases} 0 & dist_{on} - 300ms < t < dist_{on} + t_p \\ -h_p & dist_{on} + t_p < t < dist_{on} + t_p + \tau_p \\ 0 & dist_{on} + t_p + \tau_p < t < dist_{off} + 50ms \end{cases} \quad (2.7)$$

where the free parameters were time time of pulse t_p, duration τ_p and magnitude h_p. This pulse was then processed by the E-C coupling model low pass filter, $P(s)$ for comparison with the $P(s)U_{command}$ signal calculated from Eq. 2.5, Examples of $\tilde{U}$ and $P(s)\tilde{U}$ are given in Fig. 2-7.

A range of different filtered square pulse durations (including rise and fall times), were to be searched to minimize the difference between $\tilde{U}$ and $U_{command}$.
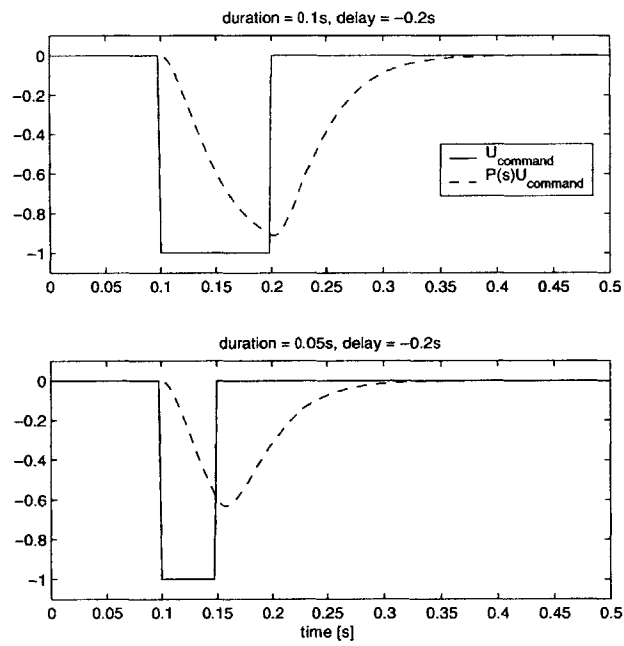
Figure 2-7: $\tilde{U}$ and $P(s)\tilde{U}$, note how rise time of the filtered signal is equal to the square pulse duration, magnitudes are one

Chapter 3

Results

The kinematic error and best fit pulse durations were studied in hopes of clarifying the control mechanism as well as the form of the feedforward command. In this section we will address each of the analysis items from Sec. 2.4.

3.1 General results

3.1.1 Data collected

Five subjects were enrolled in the study. All but one were able to perform the tasks outlined in Sec. 2.2.2 with reasonable accuracy by the end of the training session. The fifth was unable to become accustomed after the two hour training session, so was not studied. Of the remaining four subjects, one consistently encountered non-programmed forces due to mechanical malfunction of the manipulandum during the study session. Another subject was trained and tested in one session, and was not asked to do 'no resist' trials at all disturbance durations, so data from these two subjects was discarded. The analysis was therefore run on data recorded during movement blocks (B) at disturbance durations of 250, 200, 150, 125, 100 and 75ms from the remaining two subjects. One subject also did a block with 50ms disturbances.

3.1.2 Qualitative performance

Subjects initially found the tasks to be awkward, mentioning that the random disturbance onset made the requirements quite difficult by preventing the establishment of a rhythm from one trial to the next. Both completed the tasks with intense concentration. It was evident from observing the experimental sessions that the subjects had a difficult time matching the shorter disturbance durations, but both seemed to make movements with smooth velocity profiles. One subject was characteristically later in turning their force on than the other. Subjects percieved that their ability

34

to successfully counteract the disturbance in static and motion trials at a given disturbance duration were the same. Confirmation that the ability to successfully reject disturbances was not a function of state allowed us to discard the state information and save only the data from a given amount of time before, during and after the disturbance.

By observing their arm muscles it was clear that subjects were making an effort around the time that the force turned on. This effort may have been less a specific counteraction (defined as effort only in the direction counter to the disturbance) and more an indiscriminate stiffening (equal agonist and antagonist muscle activation) at the shorter disturbance durations. Both catch trials and regular trials were used for differentiating *specific* (reject only) from *nonspecific* (stiffening) efforts. Catch trials in the longer disturbance blocks showed, indeed, that the subjects were producing counteractive forces that were approximately equal in duration, onset and magnitude to the disturbance. However, viewing the hand-arm plant as a simple mass, we expect its displacement to change roughly in proportion to the square of the disturbance duration, rendering kinematic analysis of catch trials during the shorter disturbances less effective as it was difficult to distinguish between specific force counteraction and nonspecific stiffening. For these trials the dynamic data was helpful.

3.1.3 Quantitative performance

The feedforward force command, $U_{command}$, was calculated according to Eq. 2.5 using subjects' experimental data. Dynamics from 1500ms before to around 300ms before the disturbance were highly correlated with the kinematic data and matched the a priori expectations for the gross signal dynamics. This is to say that $U_{command}$ was close to zero before the pulse, and when the pulse occurred it did so at the predicted time relative to the disturbance with the expected strength and duration. However, during the disturbance $U_{command}$ reliably showed two short peaks that could not be accounted for with the model and were problematic in analysis of trials that were disturbed by short force pulses. After the disturbance, even though the subject generally did not make much plus or minus x motion, the signal often settled at a positive, nonzero, value. One subject's $U_{command}$ was generally more 'noisy' than the other at all durations, but had the same general form. The calculated $U_{command}$ from both subjects tended to become more noisy at the shorter disturbance durations.

Specific force rejection would result in a $U_{command}$ pulse in the specified direction. Because the model used here does not differentiate between agonist and antagonist commands, the $U_{command}$ from a trial in which the subject was stiffening would be zero as the net directional command is zero. Trials disturbed by short force pulses and whosel kinematic data showed little movement generally resulted in a $U_{command}$ that was small, but nonzero. This was generally interpreted as high, but not exactly equal, activation of agonist and antagonist muscles, almost a specified stiffening. On the other hand, it was clear from the dynamic data from trials disturbed by longer force pulses whether

35

the subject was specifically rejecting or generally stiffening.

Having discussed the shortfalls of the model, below (Sec. 3.3.3) we will discuss the shortfalls of the fitting algorithm. The problems encountered were simple to interpret and will be classified as one of six errors.

3.2 Kinematic analysis

Data from block B, motion trials, was analyzed. The velocity profiles of the subjects' kinematic data were relatively smooth, so we know at least that the two components of the task, movement and perpendicular force rejection, were successfully merged. The is not enough to say that the subjects were employing state based methods for both tasks, but this option is less likely due to the obvious force-time correlation and nonexisting force-state correlation.

3.2.1 Mechanical parameters

The literature describing arm impedance ([5], [12]) typically finds values of effective viscosity to be approximately one tenth that of stiffness. The values found in this study are consistent with this concept, as shown in Table 3.1. If one considers the x displacement to primarily displace the shoulder, then the moment arm was in the range r = 0.35-0.55[m]. Hence, the rotational stiffness values

$$R \left[\frac{N \cdot m}{rad} \right] = K \left[\frac{N}{m} \right] \times r^2 [m^2] \left[\frac{1}{rad} \right]$$

viscosity values

$$D \left[\frac{N \cdot m}{rad \cdot sec} \right] = B \left[\frac{N}{m \cdot sec} \right] \times r^2 [m^2] \left[\frac{1}{rad} \right]$$

and inertial values

$$H \left[\frac{N \cdot m \cdot s^2}{rad} \right] = M \, [kg] \times r^2 [m^2] \left[\frac{1}{rad} \right]$$

were for the most part within the ranges seen in the literature:

$$15 \leq R \leq 30 \quad \Leftrightarrow \quad 74 \leq K \leq 148$$

$$1.5 \leq D \leq 3 \quad \Leftrightarrow \quad 7 \leq B \leq 15$$

$$0.4 \leq H \leq 0.6 \quad \Leftrightarrow \quad 2 \leq M \leq 3$$

Except for some outlier values (in particular the low stiffness estimate at the 250ms disturbance, high viscosity at the 75ms disturbance and slightly high mass estimate at the 200ms disturbance for subject *jhl*, and for subject *jla* high viscosity estimates for the 125 and 75ms disturbances and slightly high mass estimate at the 125ms disturbance duration) the model estimates of impedance

36

disturbance duration	jhl			jla		
	stiffness	viscosity	mass	stiffness	viscosity	mass
250	56.52	7.44	3.60	81.91	5.07	3.23
200	134.23	6.23	6.43	56.78	8.72	2.40
150	80.79	1.93	4.62	84.44	9.38	3.47
125	99.07	2.60	4.66	153.21	59.38	6.84
100	102.17	5.26	3.97	83.79	10.18	3.22
75	117.79	39.23	4.14	73.51	26.85	2.61
50	101.01	6.16	4.13			

Table 3.1: Mechanical parameters for each subject

	α_1	α_2	α_3	α_4	α_5	γ	f	p	ρ
jla	0.3	0.4	0.1	0.01	1.0	0.65	0.3	0.3	40
jhl	0.3	0.4	0.1	0.01	0.2	0.45	0.3	0.4	40
spinocerebral delay						10ms			
peripheral delay						10ms			

Table 3.2: Neural parameters from Eq. 2.5 and Fig. 2-4 for each subject

are reasonable. Note that the findings in Table 3.1 are an average of the three 'no resist' trials at each disturbance duration.

3.2.2 Neural parameters

The neural parameters that resulted in the smallest residual $U_{command}$ were very close for the two subjects. The values are shown in Table 3.2 and were found by trial and error methods beginning at known reasonable values. Note, the search was only based from one set of parameters and the local minimum attained may not have been the global minimum. The contribution of the force feedback signal was an order of magnitude less than the other signals (compare α_4 with α_1, α_2, α_3 and p). The delays were determined by the signal's anatomic origin and destination, their values are shown in Fig. 2-4 and repeated in Table 3.2. Values of p, the differentiator gain of muscle spindles was estimated at around 0.1 in Hasan's study [9], but here the model was best fit with values 3 and 4 times that magnitude.

3.2.3 Qualitative performance analysis and classification

Analysis of the kinematic data provided an indication of how well the subject was completing the task. As it was difficult for subjects to align their efforts with the task's temporal requirements, Figure 3-1 indicates the possibilities of onsets and durations that might have occurred. The lines indicate the regions in which the subject was creating a counterforce to the disturbance. Note that
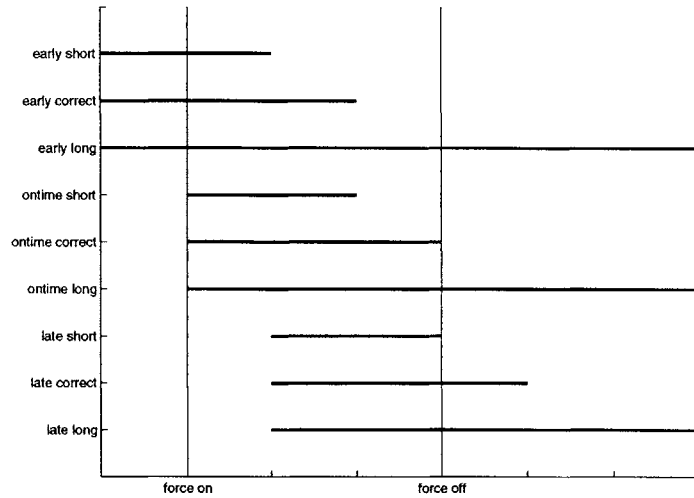
Figure 3-1: Force resist onset and duration possibilities. Lines indicate when the force is being applied

timing of subjects' efforts was not the only variable affecting succesful disturbance rejection. Some of the tirals were most consistent with an 'insufficient effort' (Fig. 3-2) and were classified as such. 'Excessive effort' was never observed.

Effort *before* the force period

If the subject began his or her force before the disturbance turned on ('force on' in Fig. 3-1) then leftward (minus x direction) movement was present at this time. If not, the trajectory would not have displacement along the horizontal axis (it was never seen that the subject created forces opposite the desired direction, ie in the positive x direction).

Effort *after* the force period

If the subject's force extended beyond the disturbance period ('force off' in Fig. 3-1), again, their trajectory would move in the minus x direction at that time.

Effort *during* the force period

During the disturbance period, if the subject was not creating a counterdisturbance their trajectory would move to the right, in the positive x direction. At this point it becomes necessary to differentiate between subject generated forces that did and did not attain the target magnitudes. If the subject's force was too weak while the disturbance was on, his or her position would increase in the x direction, but to a lesser degree than it would if they were not making an effort at all. If their force is too strong, slight leftward, minus x, movement would ensue. If the subject created the prescribed force, their trajectory would not veer from the y axis.

After examination of all the kinematic data, six representative categories were established as

Qualitative performance classifications				
DURATION	STRENGTH	EARLY	ON TIME	LATE
short	weak	Fig. 3-5	Fig. 3-2	Fig. 3-2
short	correct	Fig. 3-5	Fig. 3-4	Fig. 3-2
short	strong	Fig. 3-5	*	*
correct	weak	Fig. 3-5	Fig. 3-2	Fig. 3-6
correct	correct	Fig. 3-5	Fig. 3-7	Fig. 3-6
correct	strong	*	*	Fig. 3-6
long	weak	Fig. 3-5	Fig. 3-4	Fig. 3-6
long	correct	Fig. 3-3	Fig. 3-7	Fig. 3-6
long	strong	Fig. 3-3	Fig. 3-7	Fig. 3-6

* this scenario was presumably not seen in the data
** otherwise the subject didn't try (Fig. 3-2)

Table 3.3: Qualitative classification of subject's force resistance efforts and reference to a sample figure. Either early, ontime or late, too short, correct duration or too long, and too weak, correct strength or too strong

summarized in Table 3.3. Each trial was classified into one category according to it's most dominant compensation effect. Because it was sometimes difficult to determine on the basis of kinematics alone whether a motion was due to one of the six classifications the categorization was reevaluated later when $U_{command}$ was calculated.

Figures 3-2 through 3-7 are sample trajectories from both subjects which illustrate typical trajectories from each of the six categories: insufficient effort, long, short, early, late and good.
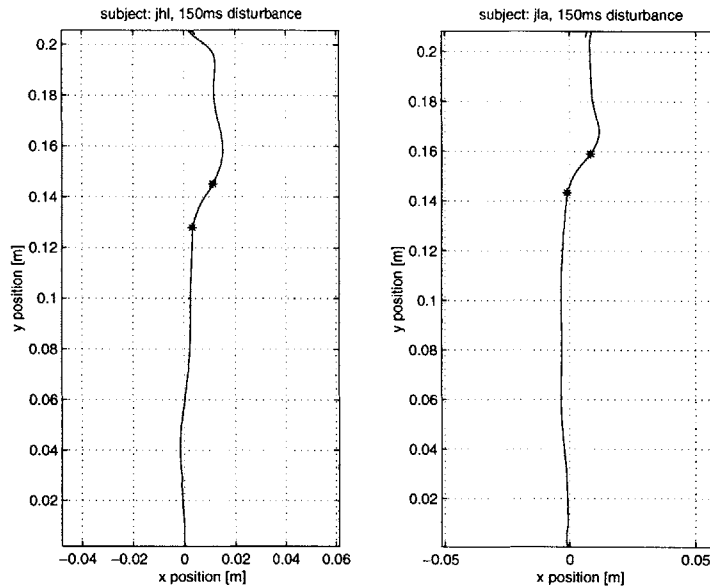
Figure 3-2: Insufficient effort: characterized by positive x direction movement as the disturbance comes on, and no negative x motion immediately following the disturbance turning off
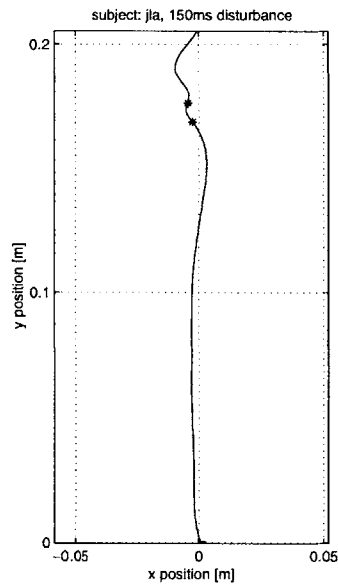

Figure 3-3: Too long: characterized by negative x motion immediately before and after the disturbance
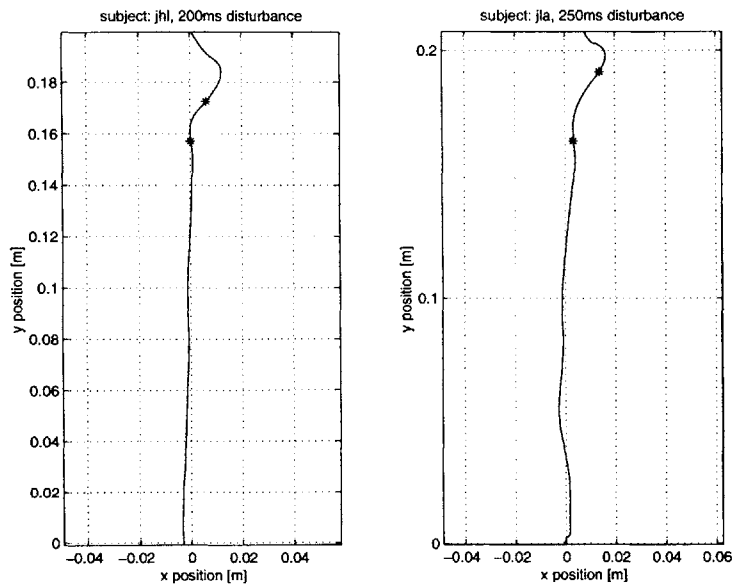
Figure 3-4: Too short: characterized by the lack of positive x motion right as the disturbance turns on, but positive x motion later in the disturbance period

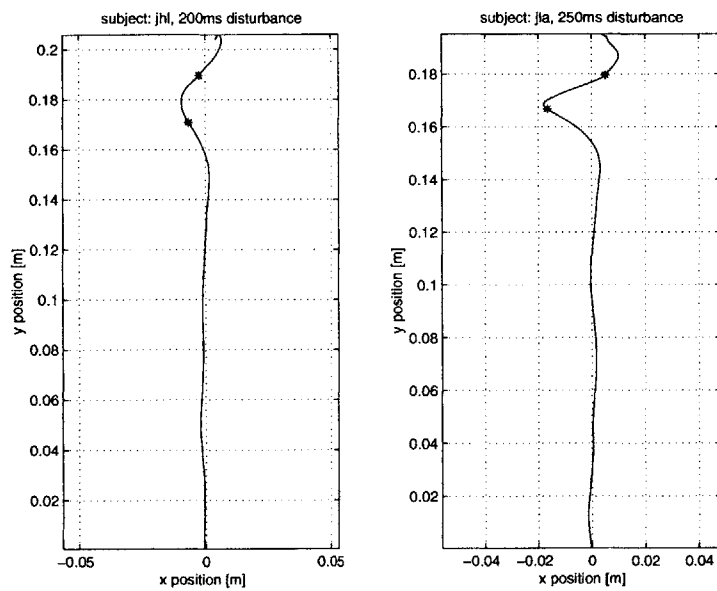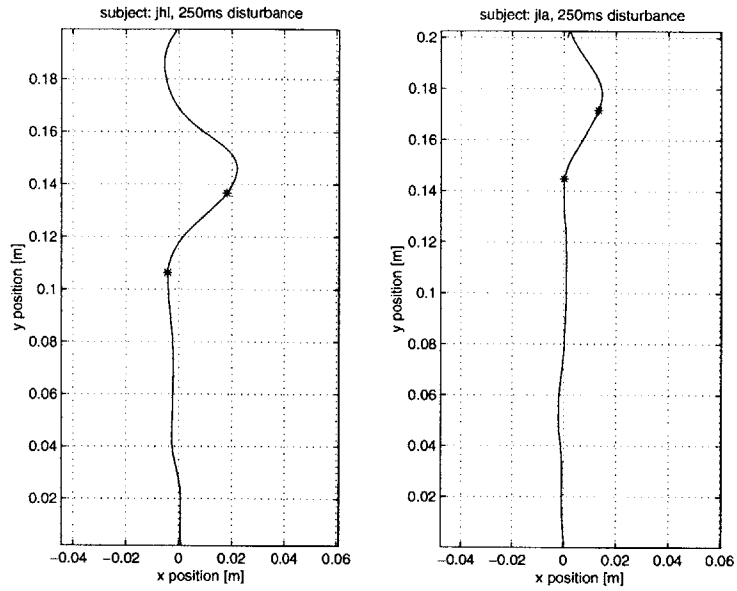Figure 3-5: Too early: characterized by negative x motion before the onset of the disturbance

Figure 3-6: Too late: characterized by positive x motion right as the disturbance turns on and negative x motion right as the disturbance turns off
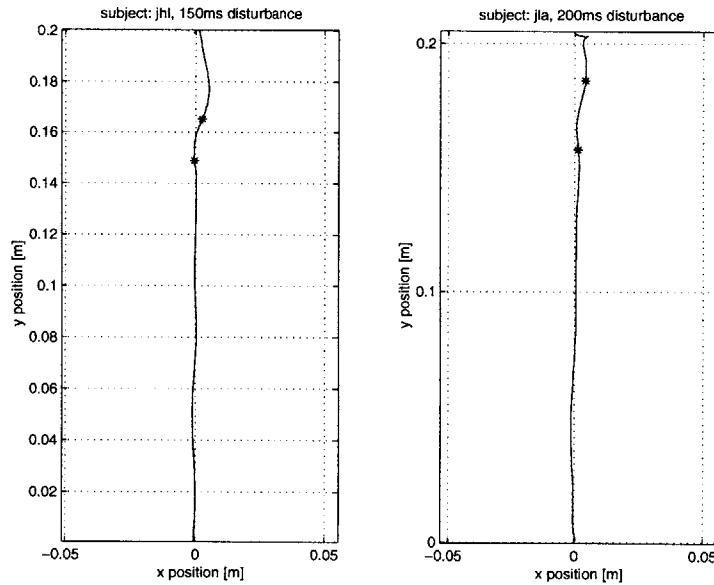

Figure 3-7: Good: characterized by little x direction movement slightly before, during and slightly after the disturbance period
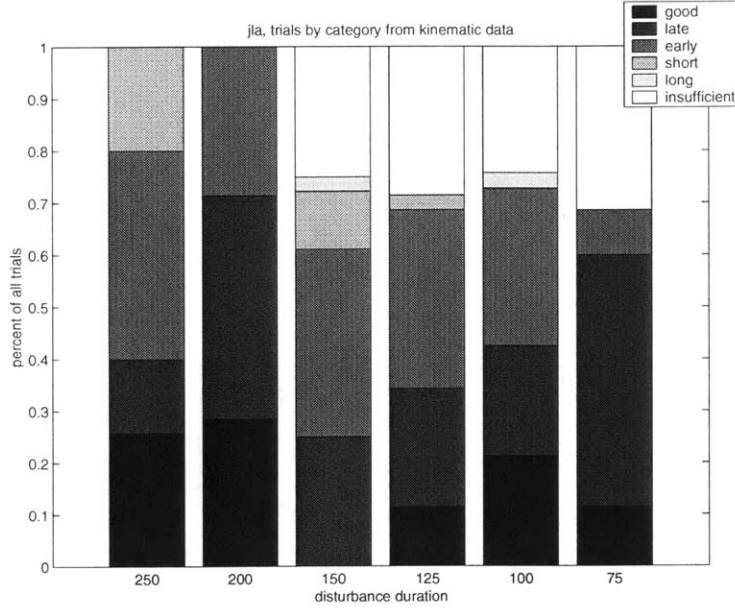
Figure 3-8: Subject: jla, classification of kinematic data by disturbance duration

In Figs. 3-8 and 3-9 the classification of all trials for each disturbance duration are plotted. The shaded bars represent the dominant effects which are mutually exclusive and therefore add up to 100%.

3.2.4 Quantitative analysis of kinematic performance

Figure 3-10 shows the subject's performances for each disturbance duration (one set of axes for each). We defined a kinematic performance index I_{kin} which represents the fraction of x-component squared velocity that was eliminated by the effort.

$$I_{kin} = 1 - \frac{\int \dot{x}^2_{error-resist} dt}{\int \dot{x}^2_{error-no-resist} dt}$$

I_{kin} was designed with the goal of adjusting for different durations and performance categories. This is to say that a large number of high error reduction trials should not be explained by a correspondingly large number of, say, 'early' trials. Results of this analysis were sorted into ten equally spaced bins (x-axis) and the number of trials in each bin is plotted vertically.

Because the subjects' normalized velocity error was similar, their data was pooled together and t-tests were run. As expected from a visual analysis of Fig. 3-10, the mean error of 250 and 150ms trials was not significantly different (significance level 0.05), similarly for 200ms and 100ms disturbance duration trials. At a significance level of 0.01, the pairs 250-75, 250-125 and 150-75 did not have significantly different means either. Table 3.4 summarizes the results of this analysis.

43
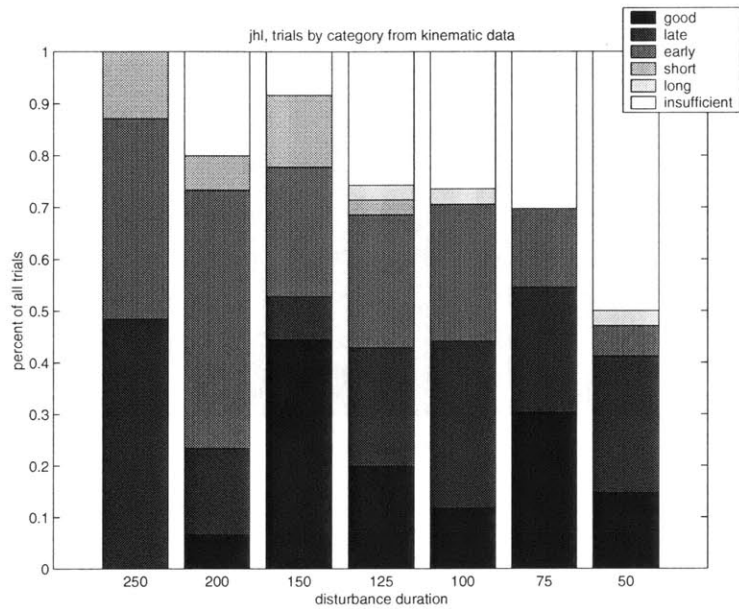
Figure 3-9: Subject: jhl, classification of kinematic data by disturbance duration

disturbance durations	250ms	200ms	150ms	125ms	100ms
75ms	3.94e-2 *	1.54e-7 *	4.52e-2 *	7.93e-1	5.36e-7 *
100ms	1.29e-3 *	4.37e-1	4.03e-5 *	3.90e-8 *	
125ms	1.17e-2 *	1.49e-9 *	8.37e-3 *		
150ms	6.09e-1	2.62e-5 *			
200ms	2.51e-3 *		* significantly different means		

Table 3.4: p-values from pairwise t-tests for different combinations of disturbance duration (two subject's data was merged)
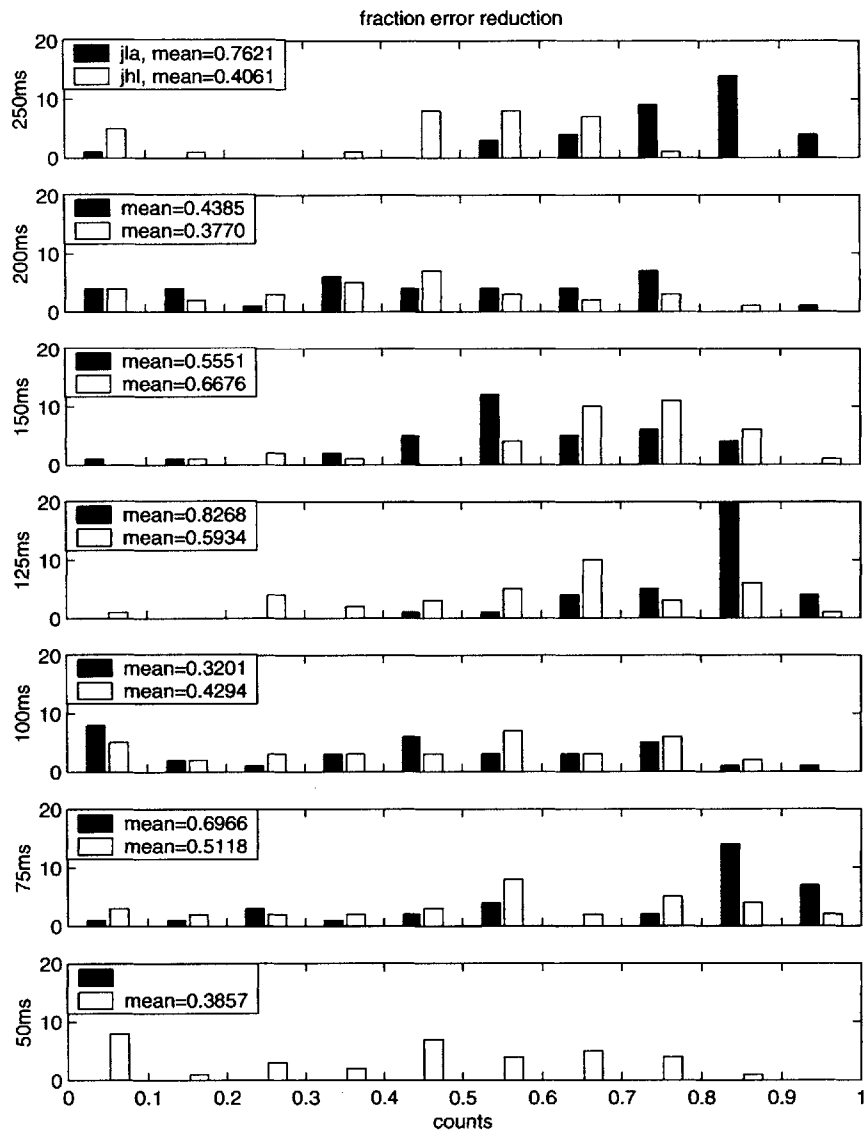
Figure 3-10: Integrated squared velocity error during 'resist' trials as a fraction of integrated squared velocity error during 'no resist' trials for each disturbance duration and subject

Figure 3-11: Components of 'no resist' trial $U_{command}$

3.3 Dynamic analysis

3.3.1 Model signal components and residual in 'no resist' trials

Figure 3-11 shows the signals used to calculate U_{resid} for the 'no resist' trials. The heavy black line is U_{resid} which was retained as a component of the model to calculate $U_{command}$. The equation for U_{resid} follows directly from Eq. 2.6:
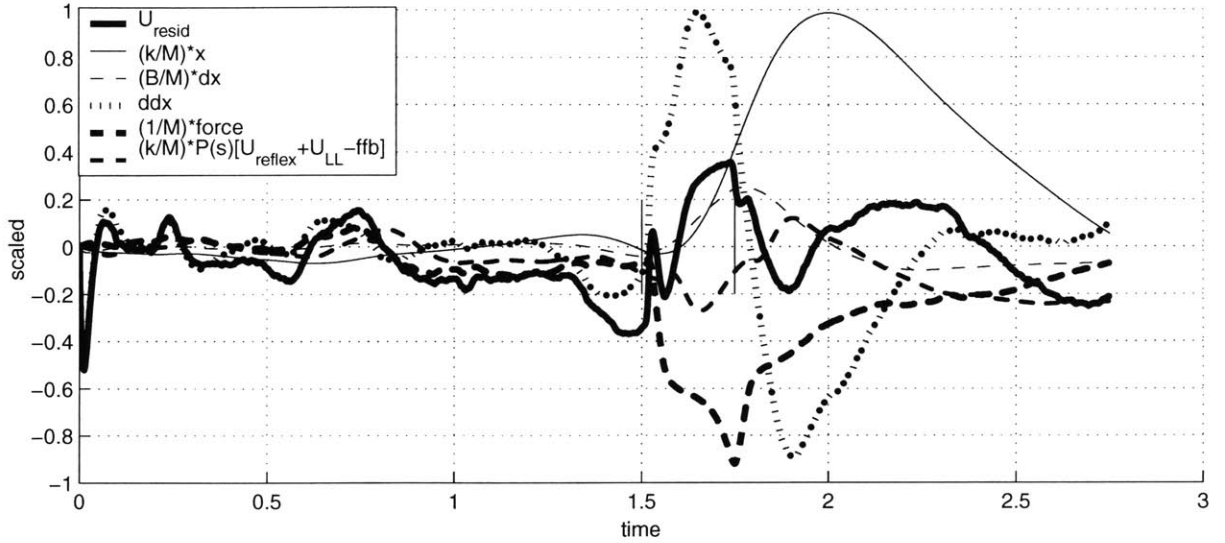
$$U_{resid} = \ddot{x} + \frac{B}{M}\dot{x} + \frac{K}{M}x - \frac{K}{M}P(s)[U_{reflex} + U_{LL} - \text{ffb}] + \frac{1}{M}F_{dist}$$

When tuning the parameters to minimize the residual $U_{command}$ in 'no resist' trials, the constrained optimization algorithm failed to significantly modify the hand selected neural parameters. While the R^2 values of the linear least squares fit of $U_{command}$ during 'no resist' trials were high (> 0.90), two characteristic peaks were apparent in *all* trials. It was not clear if this phenomenon was attributable to modeling a two joint system as a linear system, or other modeling inadequacies. Therefore, because the residual appeared to be systematic we chose to include it in the equation used to calculate $U_{command}$.

3.3.2 Qualitative features of calculated $U_{command}$ and performance reclassification

It was proposed that a reference trajectory (x_{ref}) control the movement requirements and the $U_{command}$ signal be employed in the perpendicular force control. Therefore $U_{command}$ was expected
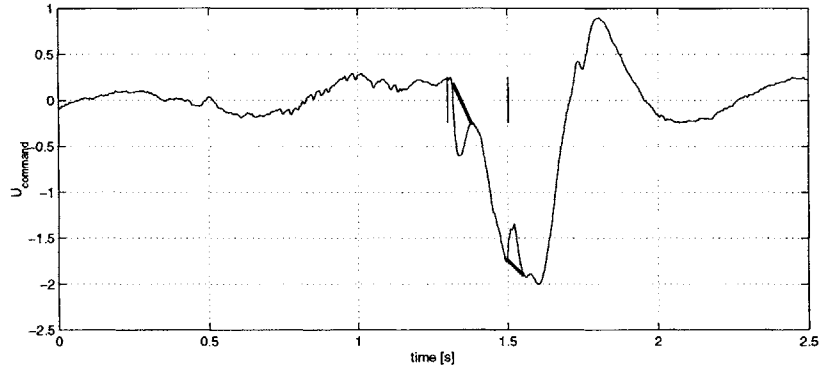
46

Figure 3-12: Peaks associated with the disturbance turning on and off during a 'resist' trial. Heavy lines indicate what the underlying signal *probably* was

to be nonzero *only* as the subject was generating their counterdisturbance. As the disturbance was aimed in the positive x direction, $U_{command}$ was expected to be in the negative x direction. Figure 3-13 shows the calculated $U_{command}$ (Eq. 2.5 with an additional $-U_{resid}$ - that would need to be scaled by $\frac{M}{K}$ - taken from the right hand side) from a sample 'resist' trial in relation to U_{LL}, U_{reflex} and *ffb*. One can readily observe that, as expected, the signal has a small amount of noise, but is approximately zero before the force rejection effort is made. In accordance with the timing of the counterforce pulse predicted from the kinematic data, a large, monophasic deflection is evident which we *presume* to represent $U_{command}$. Following the pulse are a couple of larger fluxuations in $U_{command}$, which are not evident in the kinematic data and are presumed to indicate modeling error. That the magnitude of $U_{command}$ is significantly greater than U_{LL} and U_{reflex} fits with our proposal that long and short loop mechanisms are of comparatively minor importance in this task relative to the feedforward explicit force control command. The definite form of $U_{command}$ leads us to believe that the signal is not noise.

We had expected a certain form for $U_{command}$. In general, we usually saw a monophasic pulse in the negative x direction that was interpreted as consistent with an explicit force command. We used this to refine our interpretation of the qualitative compensation patterns defined in Sec. 3.2.3. Figures 3-14 through 3-25 show representative trials from each of the categories. The dotted line represents $\tilde{U}$, the estimate of $U_{command}$ defined in Eq. 2.7 that will be discussed further in Sec. 3.3.3. Even though U_{resid} was subtracted from the calculated $U_{command}$ for 'resist' trials, the peaks were still evident as shown in Figure 3-12. However, the presence of these features was consistent for each subject at each disturbance duration, so were ignored in the dynamic analysis.

With these hypotheses in mind, $U_{command}$ signals from each trial were reclassified into the six categories. These results are shown graphically in Figs. 3-26 and 3-27. The discrepencies between these figures and Figs. 3-8 and 3-9 were generally explained by:

47
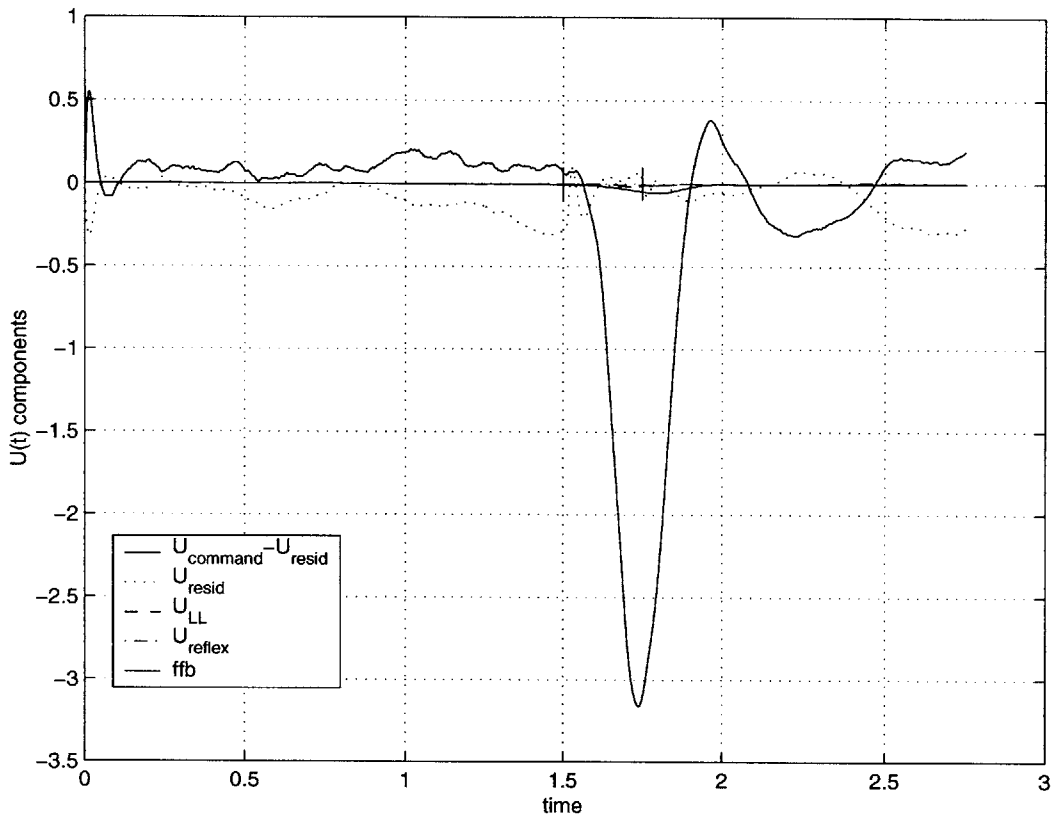
Figure 3-13: The U(t) signal (Eq. 2.4) for a sample 'resist' trial, broken up according to its components; $U_{command}$, U_{LL}, U_{reflex} and *ffb*. Compare ($U_{command}$-U_{resid}) in this figure with U_{resid} in Fig. 3-11

Figure 3-14: Insufficient effort, subject: jhl. See text (Sec. 3.3.2) for description of characterization. Two vertical bars represent force on- and offset, dashed line shows $\tilde{U}$, the best fit estimate of $U_{command}$ as discussed in Sec. 3.3.3. Kinematic data is plotted above for comparison

Figure 3-15: Insufficient effort, subject: jla. See Fig. 3-14 caption for explanation

Figure 3-16: Too long, subject: jhl. See text (Sec. 3.3.2) for description of characterization. Two vertical bars represent force on- and offset, dashed line shows $\tilde{U}$, best fit estimate of $U_{command}$ as discussed in Sec. 3.3.3. Kinematic data is plotted above for comparison

Figure 3-17: Too long, subject: jla. See Fig. 3-16 caption for explanation
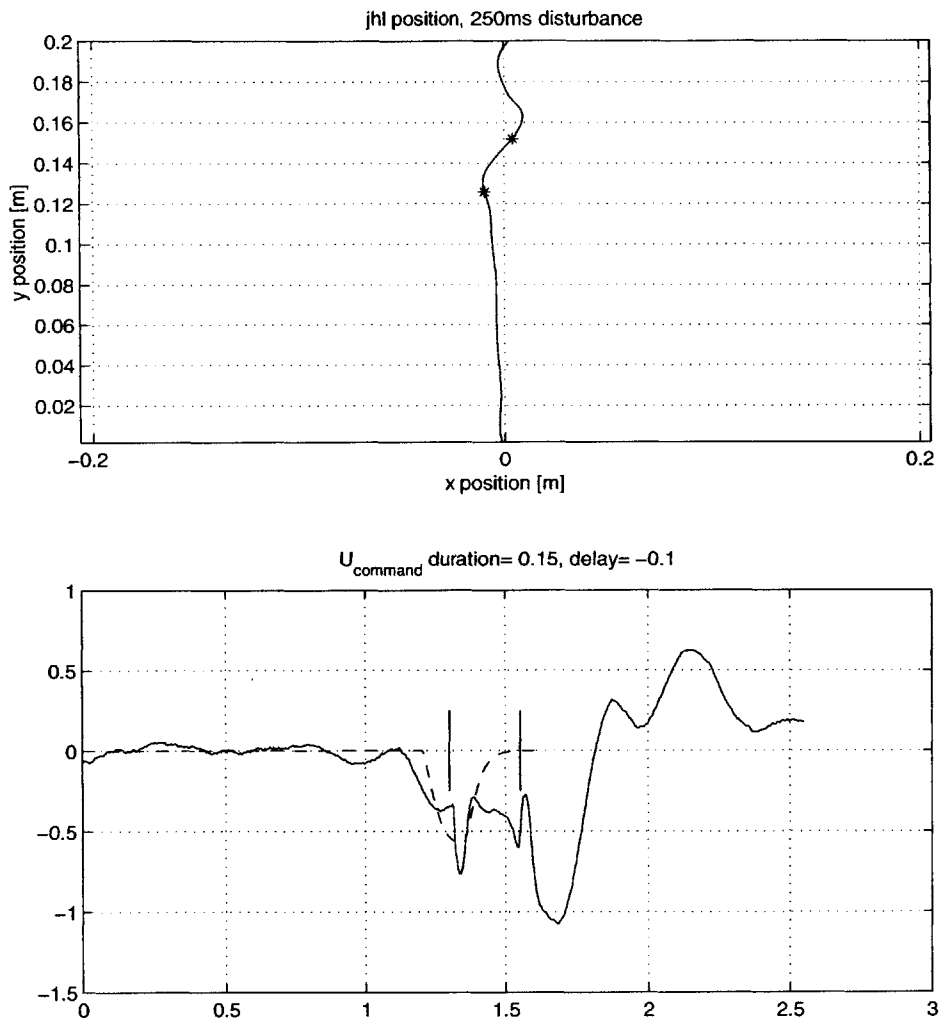
Figure 3-18: Too short, subject: jhl. See text (Sec. 3.3.2) for description of characterization. Two vertical bars represent force on- and offset, dashed line shows $\tilde{U}$, best fit estimate of $U_{command}$ as discussed in Sec. 3.3.3. Kinematic data is plotted above for comparison

jla position, 150ms disturbance

U_command duration= 0.135, delay= -0.025

Figure 3-19: Too short, subject jla. See Fig. 3-18 caption for explanation

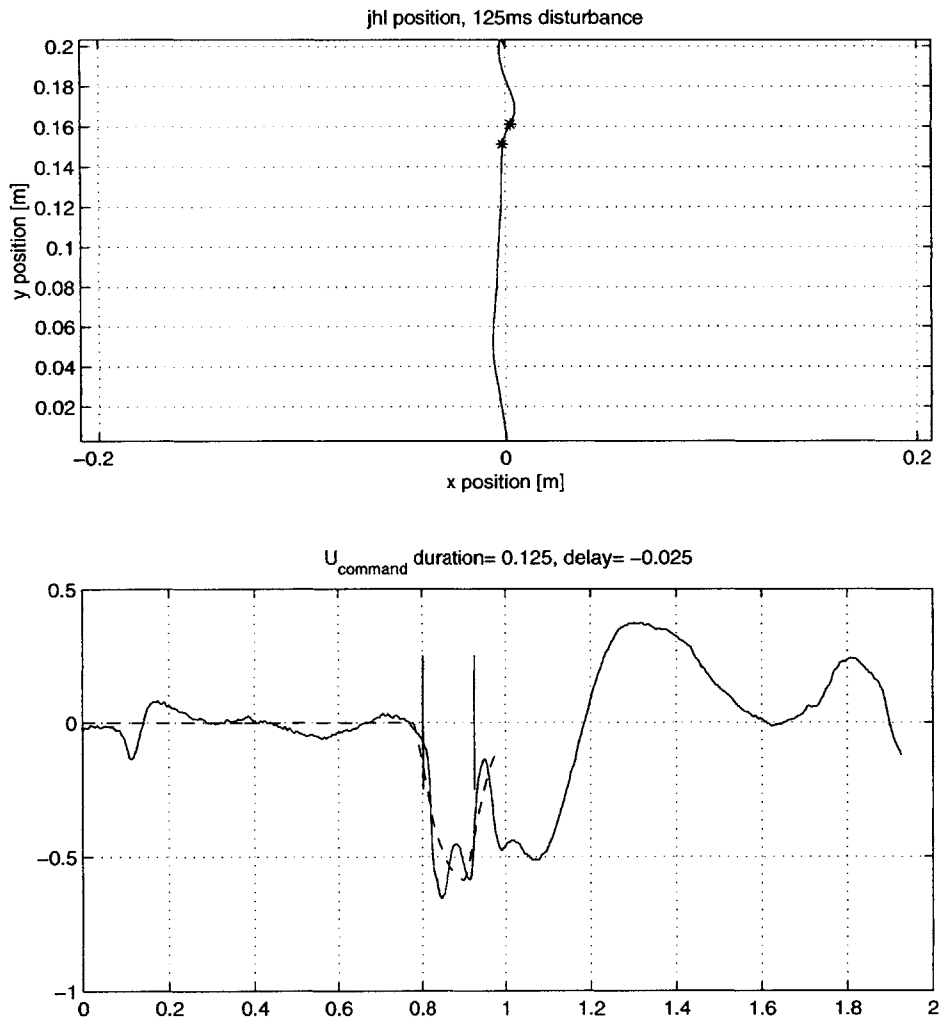**jhl position, 250ms disturbance**

U$_{command}$ duration= 0.15, delay= −0.3

Figure 3-20: Too early, subject jhl. See text (Sec. 3.3.2) for description of characterization. Two vertical bars represent force on- and offset, dashed line shows $\tilde{U}$, best fit estimate of $U_{command}$ as discussed in Sec. 3.3.3. Kinematic data is plotted above for comparison

Figure 3-21: Too early, subject jla. See Fig. 3-20 caption for explanation
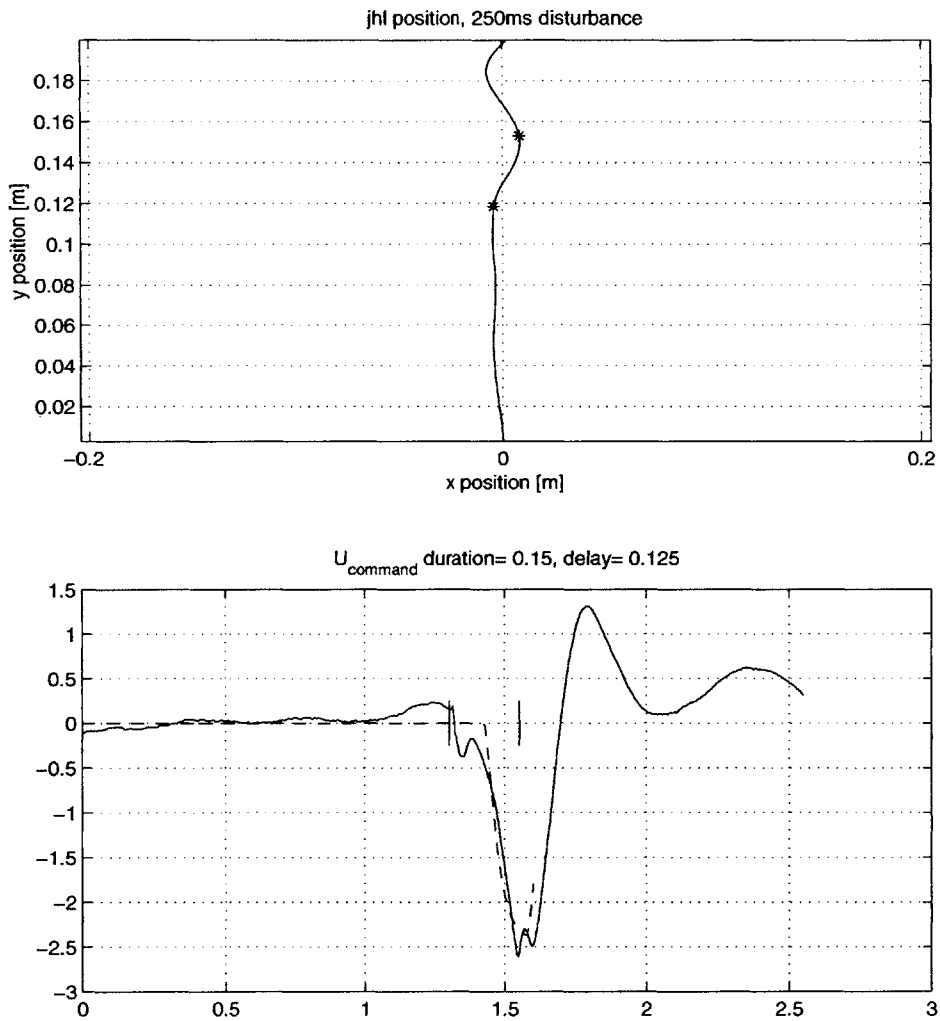
Figure 3-22: Too late, subject jhl. See text (Sec. 3.3.2) for description of characterization. Two vertical bars represent force on- and offset, dashed line shows $\bar{U}$, best fit estimate of $U_{command}$ as discussed in Sec. 3.3.3. Kinematic data is plotted above for comparison
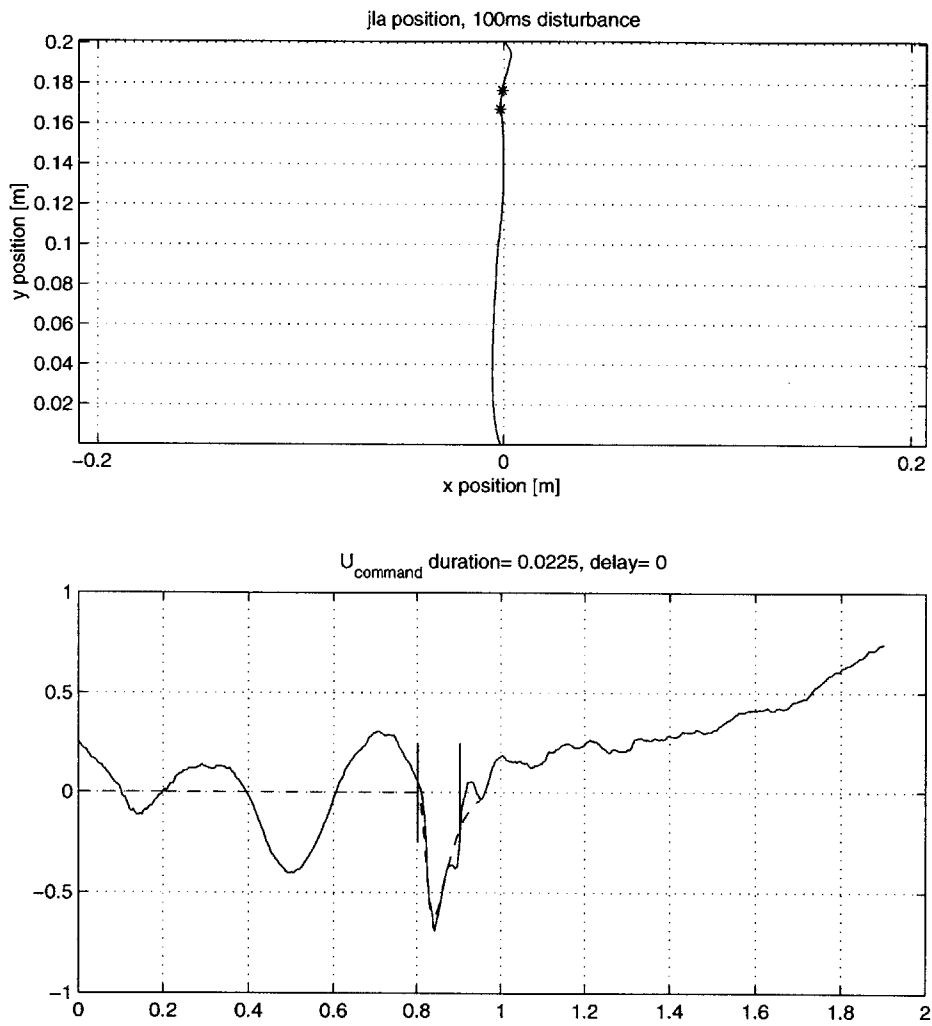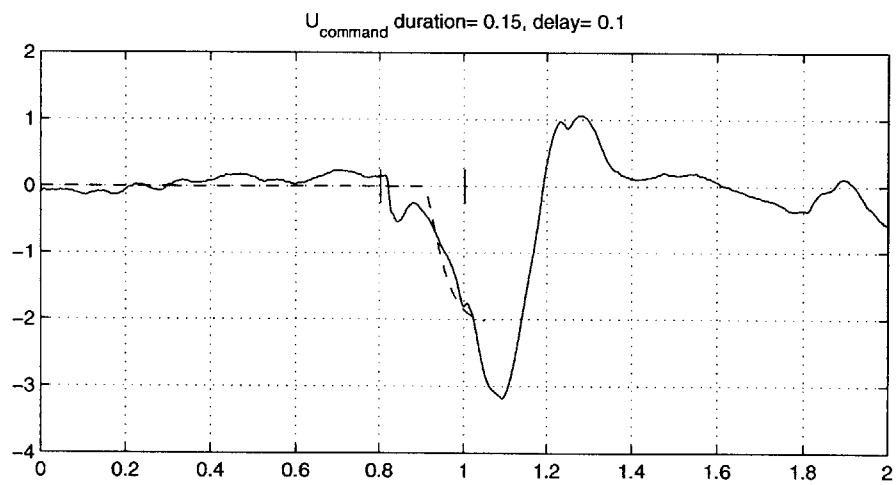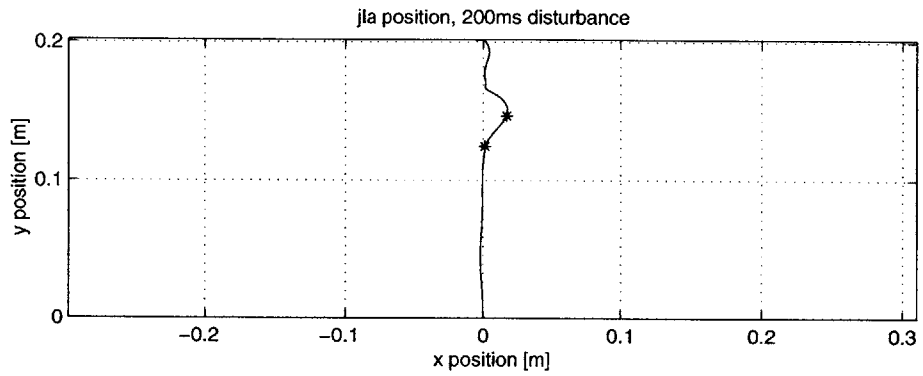
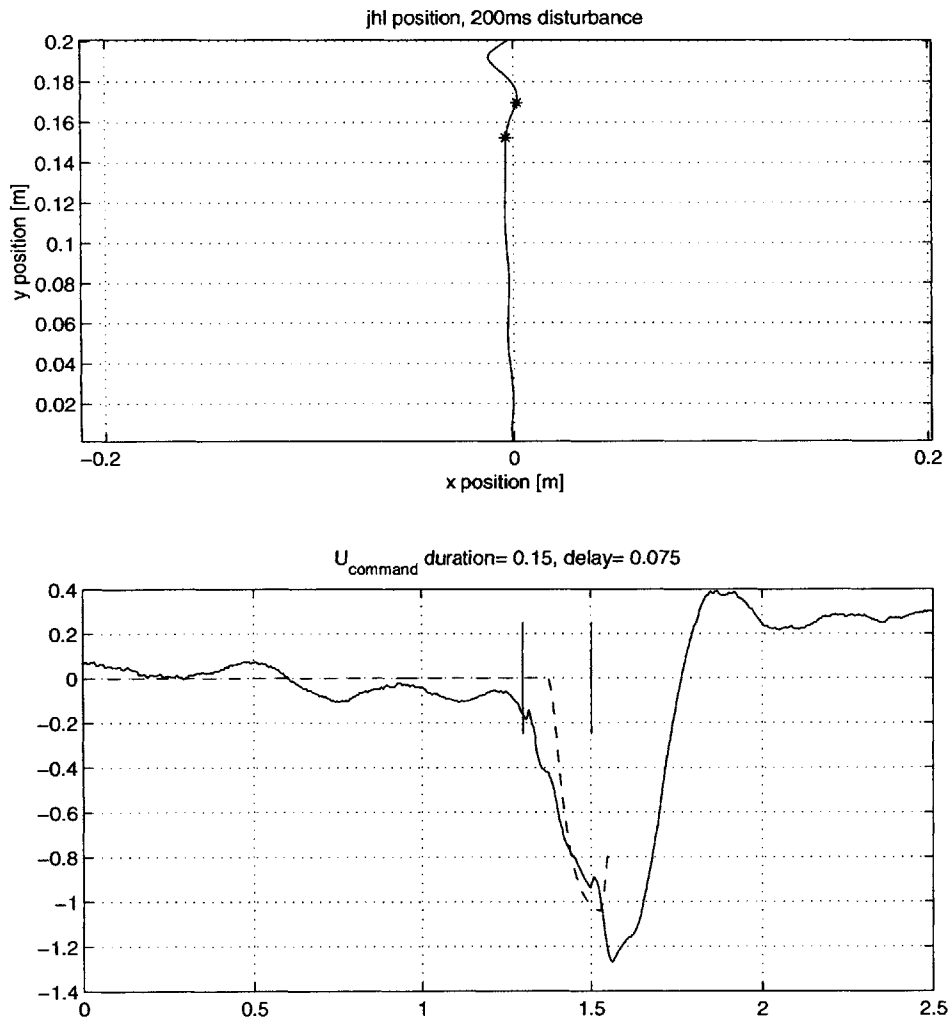Figure 3-23: Too late, subject jla. See Fig. 3-22 caption for explanation
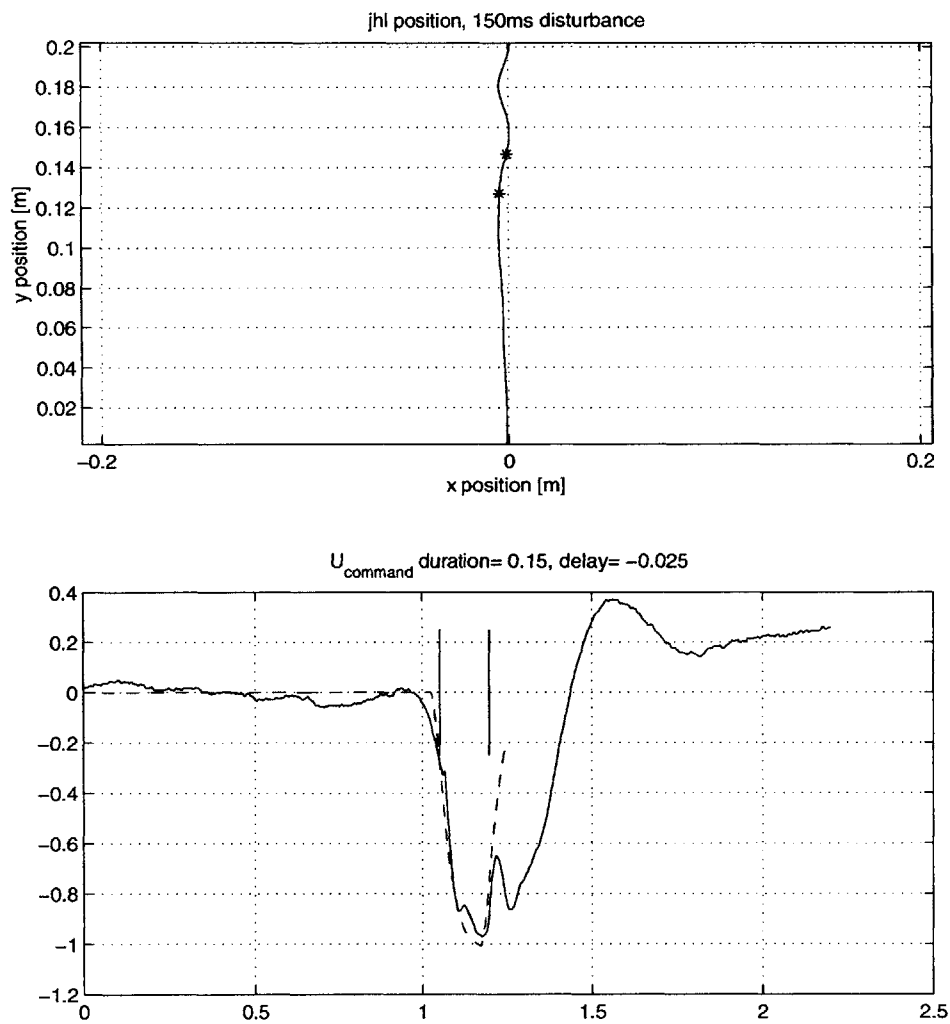
Figure 3-24: Good, subject jhl. See text (Sec. 3.3.2) for description of characterization. Two vertical bars represent force on- and offset, dashed line shows $\tilde{U}$, best fit estimate of $U_{command}$ as discussed in Sec. 3.3.3. Kinematic data is plotted above for comparison
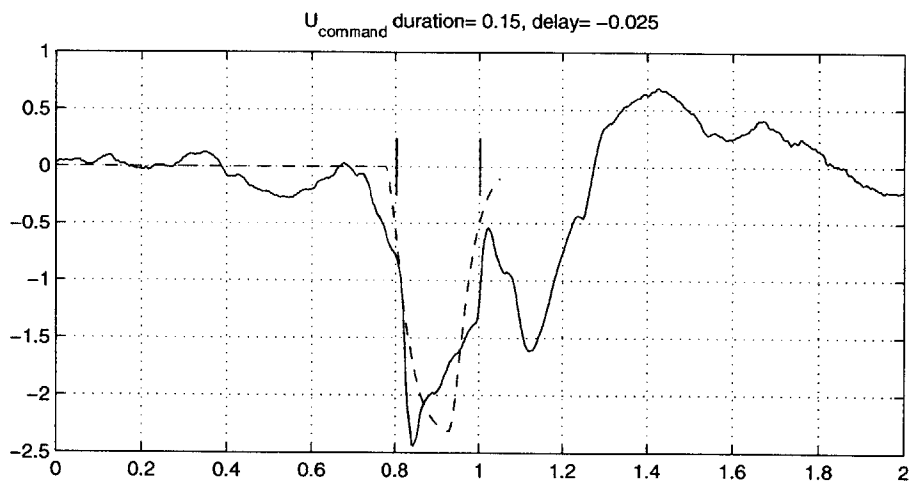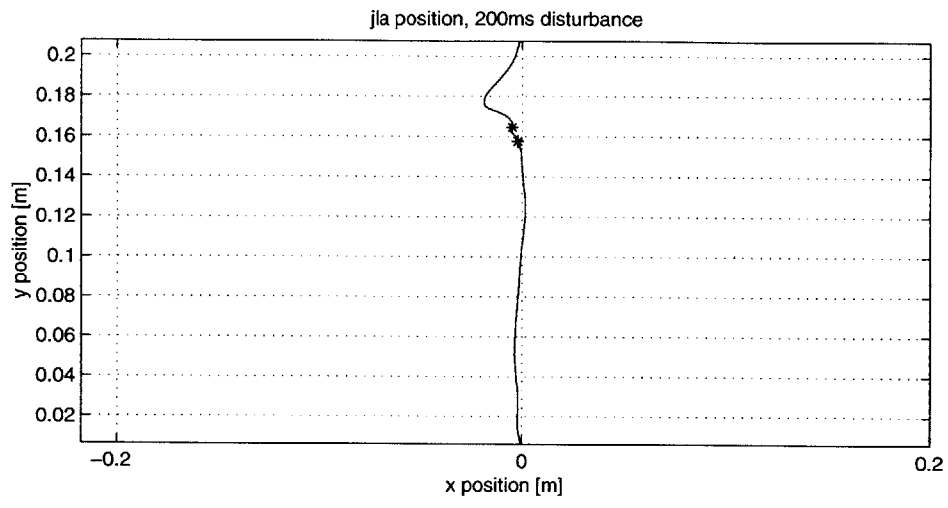
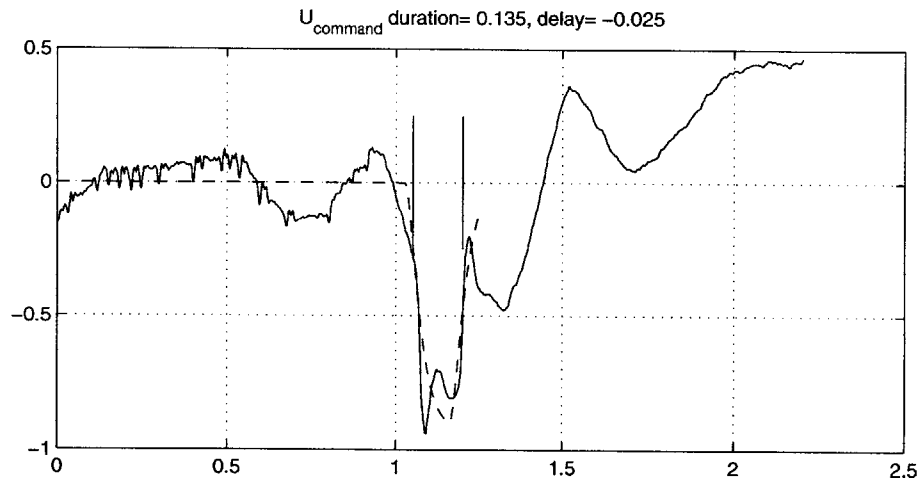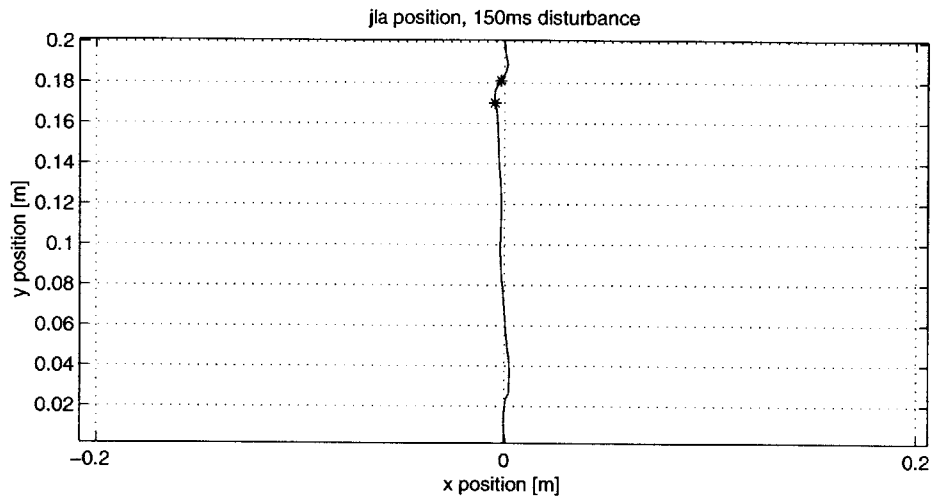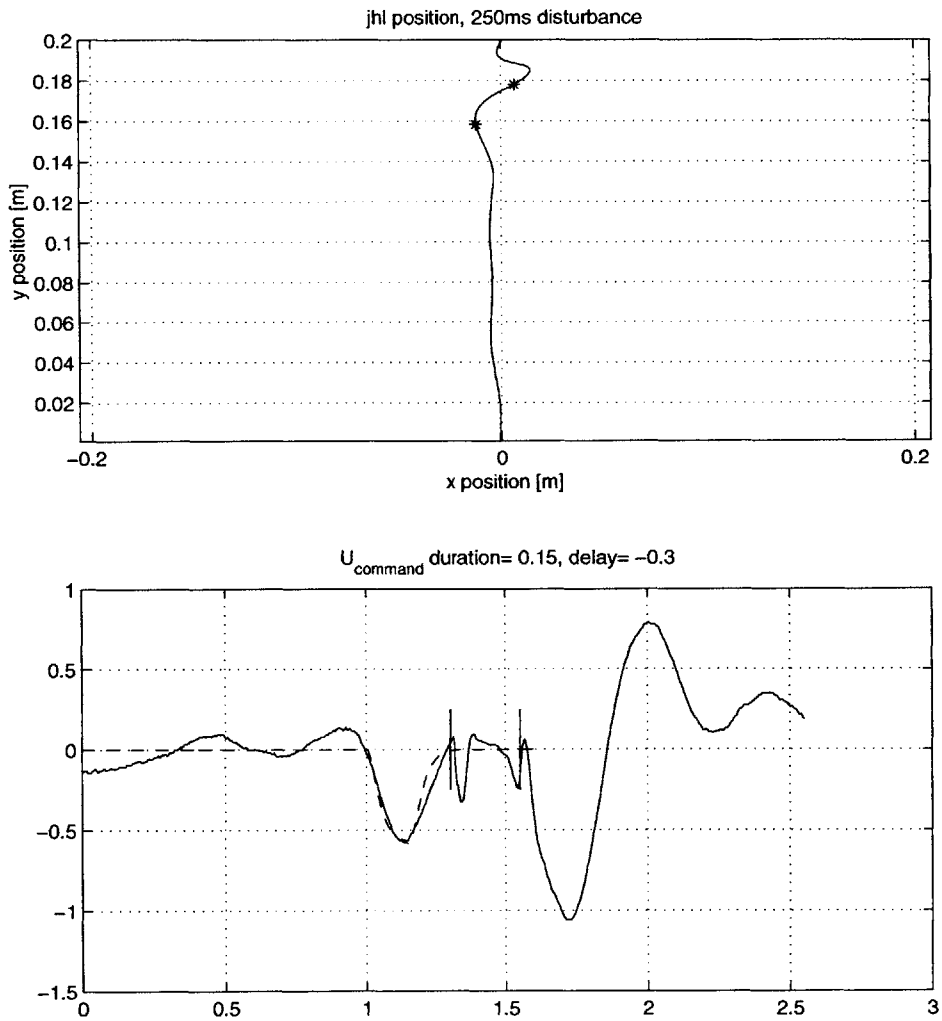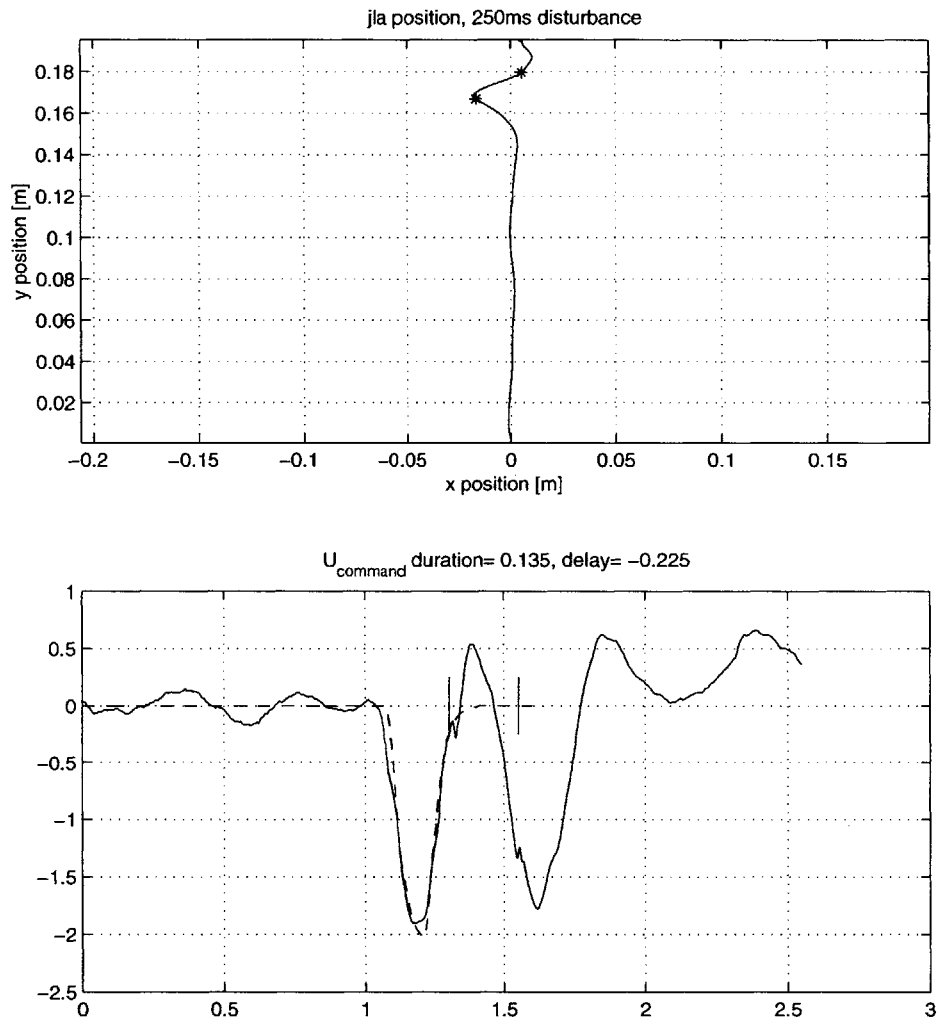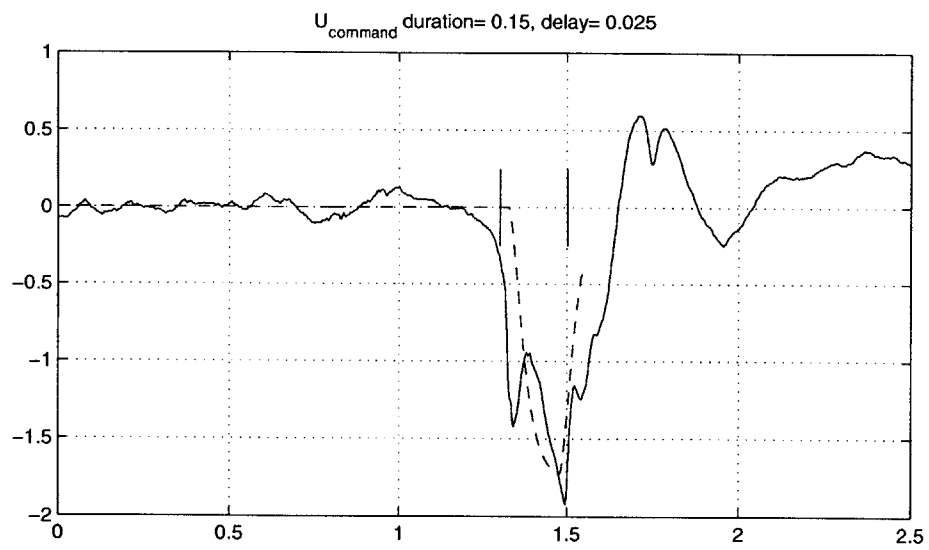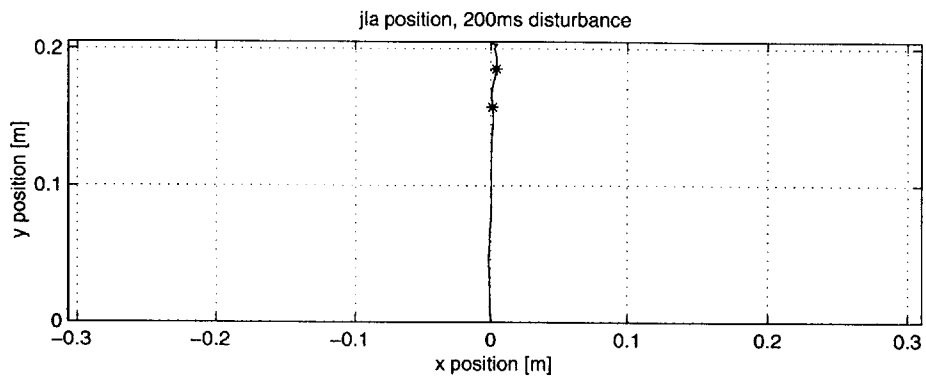Figure 3-25: Good, subject jla. See Fig. 3-24 caption for explanation
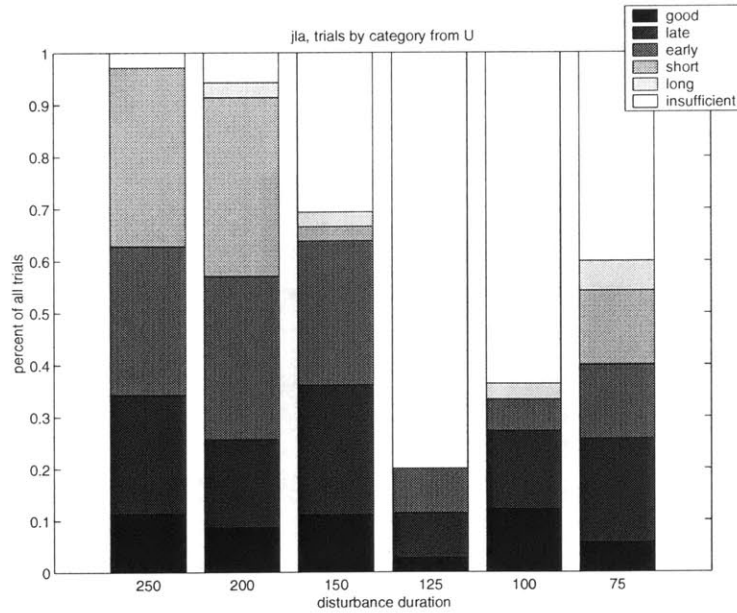
Figure 3-26: Subject: jla, reclassification of data according to $U_{command}$

- The kinematic data indicated that the subject's effort began too early, but occasionally the $U_{command}$ from those trials had only a very minor pulse that was 'too early'. In this case the trial was reclassified according to the predominant pulse in $U_{command}$.

- Often a subjects effort was bi-phasic, meaning that there were too equally compelling efforts made around the time of the disturbance. For these situations the pulse that was closer to the actual disturbance was used for categorization.

- Misclassifications arose most frequently for the short disturbance duration trials when the kinematic data showed only minor x direction motion.

When the dynamic data was being sorted into the categories, by and large it was evident why the trial was classified as it was, but the additional information made it possible to sort the trials into more appropriate categories.

3.3.3 Fitting pulse model, $\tilde{U}$ of $U_{command}$

The longest disturbance lasted 300ms. $\tilde{U}$ pulses as long as 345ms were fit to enable room for error. A qualitative analysis of the calculated $U_{command}$ indicated that there were no pulses of total duration shorter than about 200ms (when the erroneous peaks associated with the disturbance turning on and off are ignored, see Fig. 3-12). But, again, to allow room for error minimum durations as low as 125ms were tested. As one of the goals of this study was to look in detail at force pulse durations, the range was broken up into increments of 10 to 15ms. Filtered pulse $(P(s)\tilde{U})$ durations correspond to
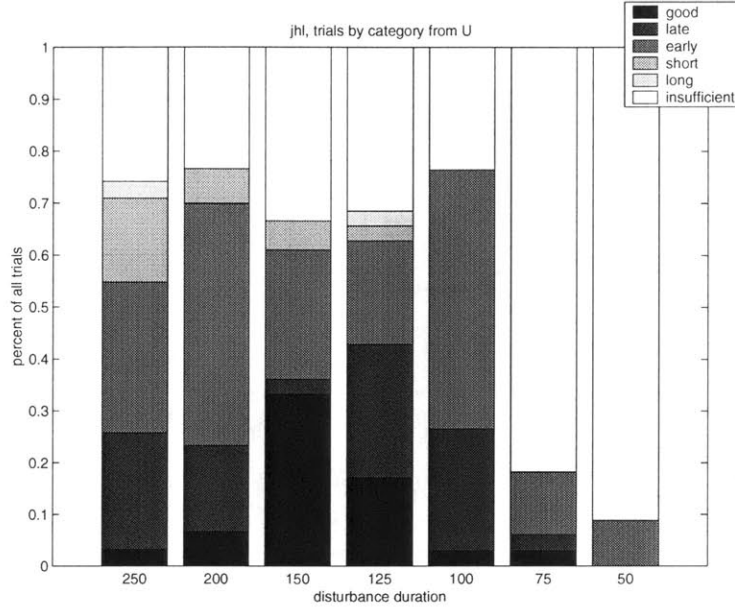
Figure 3-27: Subject: jhl, reclassification of data according to $U_{command}$

square pulse ($\tilde{U}$) durations of 2.5 to 150ms. When minimum force generation times are considered in the literature, it is generally the rise time (not the rise *and* fall time) that is being discussed. Figure 2-7 indicates that rise time is synonymous with square pulse duration, so it is this time scale that will be used in further duration analysis.

Fourteen to eighteen different delays (depending on the disturbance duration), ranging from 300ms before the disturbance onset to halfway through the disturbance period in 25ms increments were considered in finding the best fit for $U_{command}$. Subjects almost never began their rejection effort more than 300ms early. The dynamics after the disturbance were not captured in the model, so it did not make sense to attempt to fit beyond this range (50ms after the disturbance ended). The maximum allowable delay for the best fit pulse was chosen to be halfway through the disturbance with the rationale that if the subject had not began their rejection effort by this time, their efforts would be marred by the unreliable $U_{command}$. Each fit was considered individually and some were discarded as will be explained below.

At each duration/delay combination, the best fitting magnitude for the pulse was found using linear least squares regression. In some cases the magnitude was found to be negative, which would indicate that the command was opposite in direction from a disturbance cancelling command (usually this happened when there was significant left to right movement before the disturbance came on). For each trial the error,

$$\int_{\text{dist}_{on}-300ms}^{\text{dist}_{off}+50ms} (P(s)\tilde{U} - P(s)U_{command})^2 dt$$

for each duration and delay combination with positive magnitude were compared and the parameters that minimized this error were saved.

The figures showing the classification of $U_{command}$ (3-14 through 3-25) also include the best fit estimations $\tilde{U}$ as dashed lines. Problems encountered by both subjects are listed here in descending order from most to least common. The axes numbers refer to Figure 3-28.

- The fitting algorithm considered artifacts such as the peaks that were seen at disturbance on and offset to be the subject's effort. Usually this occurred if the trials were 'too late' or 'too early'. All estimations of this sort were discarded. 60% of the trials that were discarded were discarded due to this type of artifact. This was especially common during short disturbance durations where the fits were dominated by the transients at onset and offset. An example of this scenario is shown on axes 3,2.

- The algorithm searches for a pulse, and assumes that one exists. If the subject's effort was too weak the algorithm just found the most prominent pulse and these trials were saved. 13% of the trials that were considered poor fits were because the subject didn't make sufficient effort. An example of this scenario is shown on axes 2,2.

- In a few cases the pulse that the subject made was longer than the maximum 345ms pulse used in the fitting. These trials were kept for the pulse duration analysis. 12% of the poorly fit trials were due to pulses that lasted longer than the allowable duration. An example of this scenario is shown on axes 2,1.

- Subjects occasionally didn't make clean or distinct force pulses. The trials that were discarded because the fitting algorithm had come up with a pulse that was some sort of averaging of the $U_{command}$ signal. 7% of the poor fits were due to indistinct efforts. An example of this scenario is shown on axes 1,1.

- On the 'too long' trials it sometimes happened that the probable effort we were looking for was systematically ignored and the best fit pulse was delayed the maximum amount to fit stronger pulses that were most likely corrective movements. These fits were discarded as they had no relation to the feedforward command. 6% of the trials had significant corrective movements that led to poor fits. An example of this scenario is shown on axes 1,2.

- In a couple of cases the $U_{command}$ pulse was more broad than the prototypical fitted pulses. When $\tilde{U}$ had approximately the same duration as the $U_{command}$ pulse, the data was retained for the duration analysis. Discrepency in shape caused only 2% of the poor fits. An example of this scenario is shown on axes 3,1.

Because of the problems encountered in the fitting, very little of the best fit duration data from trials with disturbance durations shorter than about 125ms was reliable.
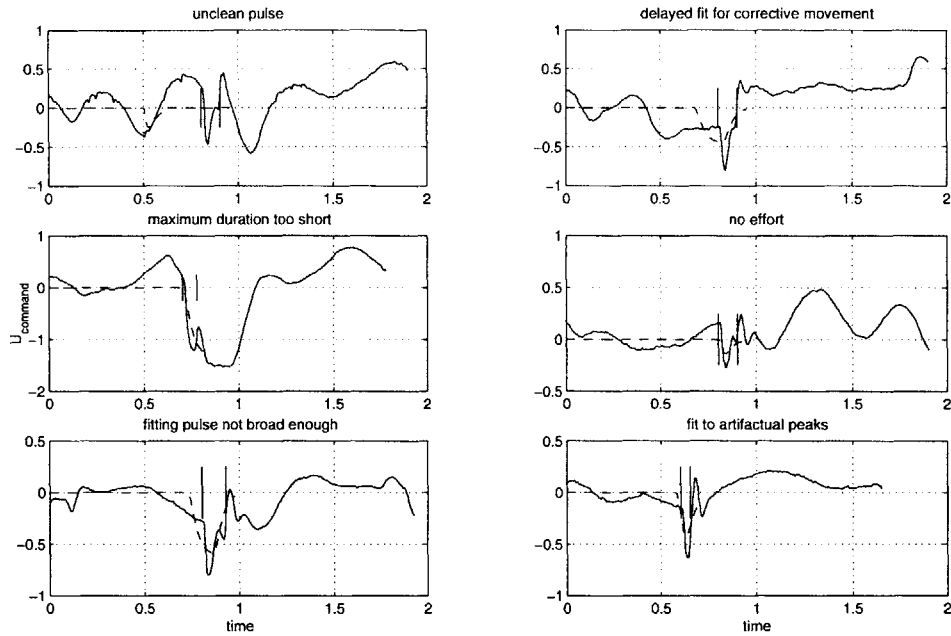
Figure 3-28: References to this figure made in the text (Sec. 3.3.3) label the axes as 'row','column' pairs

3.3.4 $\bar{U}$ pulse durations

That we were unable to reliably fit short duration efforts was wholely due to the fact that they were not observed. Clean efforts that were evident in $U_{command}$ for longer disturbance durations were either evident at the same long durations as in shorter disturbance duration trials or altogether not present. Very few trials were reliably fit with pulse durations shorter than 300ms (corresponding to rise times of 105ms, see Table 3.5), a fact which kept us from making conclusions regarding the quanization of pulses. Of the data that was kept (percentages shown in third column), counts of each possible best fit duration are shown for each disturbance duration and subject in Table 3.5. One can readily see that much of the data was discarded for the 125ms and shorter disturbance durations, but also that pulses longer than the required duration were usually made. Not shown in the table is that subject jhl's 200ms disturbance trials were reliably fit with with a pulse with rise time 2.5ms and two from the 50ms disturbance duration trials were also best fit with the 2.5ms rise time pulse. Though these fits were not artifactual, they were quite rare and therefore not interpreted to actually represent the intended $U_{command}$.

disturbance duration	subject	percent kept	best fit pulse rise times									total
			67.5	77.5	87.5	95	105	115	125	135	150	
250	jla	60.0	0	0	0	0	0	0	1	1	19	21
	jhl	54.8	0	0	0	0	0	0	1	0	16	17
200	jla	91.4	0	0	0	0	0	0	0	2	30	32
	jhl	73.3	0	0	0	0	1	0	0	2	18	21
150	jla	36.1	0	0	0	0	0	0	0	1	12	13
	jhl	74.3	0	0	0	0	0	0	1	1	24	26
125	jla	11.4	0	0	0	0	1	1	1	0	1	4
	jhl	17.1	0	0	0	0	0	1	0	3	2	6
100	jla	24.2	0	1	0	0	2	0	2	1	2	8
	jhl	14.7	0	0	0	0	0	0	1	0	4	5
75	jla	22.9	0	0	1	0	0	2	0	0	5	8
	jhl	0.0	0	0	0	0	0	0	0	0	0	0
50	jhl	5.9	0	0	0	0	0	0	0	0	0	0
		total	0	1	1	0	4	4	7	11	133	161

Table 3.5: Best fit pulse rise times by subject and disturbance duration from trials in which $\tilde{U}$ was considered a good fit (percentage of trials considered good fit shown in third column)

Chapter 4

Discussion, conclusions and future work

4.1 Adequacy of the study and central findings

In brief, the results from this study provide a good start at addressing the issue of the time domain characteristics of human force control in rejection of transient disturbances during movement. We believe that the results, if not totally complete, are reliable within the scope discussed above. The data that was fully analyzed from two subjects were generally in agreement. Namely, each subject found the task easier at longer disturbance durations and tended to stiffen rather than create specific force rejection pulses at shorter disturbance durations. The problems experienced at shorter disturbance durations were both similar and different from those experienced at longer durations. Whether the subject was early or late, or too weak or too strong did not seem to be influenced by the disturbance duration. But subjects were much more likely to create counterforces that lasted too long at shorter disturbance durations.

Here we plan to address each of the hypotheses posed earlier keeping in mind the goals of first confirming whether the proposed model can account for the arm's dynamics, and if so, trying to learn a little about the system in terms of its capabilities for force control.

4.2 Explicit time-based force command and its independence from implicit motion state based force command

We will address each compensation methods from Sec. 2.2.1 and narrow the control possiblilties according to the analysis results.

4.2.1 Stiffening

Catch trials were used to minimize stiffening during the experiments. If the investigator noticed a lack of afftereffects during a catch trial, subjects were notified and quickly corrected their behavior so that *specific* efforts were used to reject the disturbance. Still, dynamic data from some trials was classified as having 'insufficient effort', which may be explained as stiffening as the net force command against the disturbance was very small.

4.2.2 Learned functions

As the study's findings seem to indicate that the ability to reject the disturbances was independent of motion state, it can be said with relative certainty that subjects were not employing pure feedback control with the use of look-up tables. Similarly, because subjects were able, upon each interaction with a disturbance whose relation to the reference command had not been experienced before, to perform with the same accuracy as they did on exposure with forces that had been encountered previously, we can conclude that subjects were not employing error based look-up mechanisms.

4.2.3 Implicit cerebellar computation

Owing to the unattributable 'peaks' observed in the dynamic data, we were unable to confidently determine the minimum force pulse duration subjects can make. Had we determined this minimum, and found it to be no shorter than 100ms, implicit cerebellar computation would have been ruled out as it has been established that force pulses implicitly calculated in the cerebellum can be shorter than this duration.

4.2.4 Explicit time-based force command

The measures taken in designing the experimental tasks, namely randomizing the onset of the disturbance during the reaching movement and testing on a range of disturbance durations (from 'established capability' as determined in earlier studies, to 'likely infeasible' according to theoretical rationale), provided a broad scope under which to study subjects' ability to employ force control methods in disturbance rejection.

In summary, the work done here is enough to rule out stiffening and look-up tables. After determining the nature of the 'peaks' observed in $U_{command}$, these data can be estimated and the best fit durations may be compared with the literature to either conclude that the minimum force pulses are or are not below the critical 100ms duration.

4.3 Diminished performance at short disturbance durations

4.3.1 E-C filtering

Subjects encountered latency, duration and effort intensity challenges at all disturbance durations. Understanding how the E-C coupling filter, P(s), affects these variables may help us understand why problems arose. As is shown in Fig. 2-7, the filtering of shorter square pulse durations results in decreased magnitude, so that to attain the desired magnitude a pulse with greatly increased magnitude must be commanded. In addition, again especially with regard to the shorter disturbances, the rise time may be in accordance with the task, but filtering by P(s) results in a fall-off time longer than rise time which would render the effort 'too long'.

4.3.2 Quantization

Preferred pulse durations might indicate the use of subforce components depending which durations are 'preferred' and whether slightly longer *and* shorter durations are not. Therefore, velocity error reduction for the two subjects was pooled together and analyzed. The error reduction was relatively high at the 250ms, 150ms, 125ms and 75ms disturbance durations and relatively low at the 200ms, 100ms and 50ms disturbance durations (Fig. 3-10). Table 3.4 shows that statistical tests confirm the similarity of the 200ms/100ms, 250ms/150ms, and 125ms/75ms distributions. While the mean error reduction for the 200ms and 100ms trials is similar, it is not close to one, implying that subjects found the durations equally not-so-easy. On the other hand, the 250ms/150ms and 125ms/75ms trials have similar distributions of error reduction *and* the mean is relatively high. But as 250 (125) is not approximately an integral multiple of 150 (75), we cannot confidently say that subforces have 150ms (75ms) duration.

As the goal was to eventually go beyond the realm of preference and say that very short pulses are not only not preferred, they are not possible, minimum durations were studied as a mean of achieving this ends.

4.3.3 Minimum duration

Though the qualitative measures of Figs. 3-26 and 3-27 were subjective, it appears that *jhl* did the best at the 150ms disturbances and provided insufficient effort in the majority of 75 and 50ms disturbance duration trials, which does suggest a lower limit on force pulse durations. It was difficult to draw any decisive conclusions from *jla*'s qualitative data.

Durations of the best fit estimates, $\tilde{U}$ were compared. As much of the data was erroneous, full analysis was impossible. Still, the results from the reliable trials are quite interesting. Table 3.5 shows how many $U_{command}$ signals were best fit by $\tilde{U}$ with rise times of 67.5, 77.5, 87.5, 95, 105,

115, 125, 135 and 150ms. By and large, subject's data was best fit with pulses with 150ms rise time, regardless of the tasks requirement, each of these trials was considered a good fit. Trials in which the 150ms rise time was too short are not included here.

4.4 Model

Additions to Massaquoi's model [13] were the *force* feedforward and feedback control signals. As the merits of the existing model components were discussed upon its original proposal, the value of the new components will be discussed here.

4.4.1 Feedforward command

Before calculating $U_{command}$, the model was used to estimate the mechanical parameters involved using data from subjects' 'no resist' trials. These estimates were found to be consistent with other findings in the literature. Next, the model was used to backwards compute a proposed feedforward force command using 'resist trial' data. The signals that resulted bore strong resemblence to the features that were expected. In particular, if the kinematic data indicated that the subject's timing was off, $U_{command}$ indicated the very same mismatch, often times providing more information than could be obtained from the kinematic data. The relative contribution of the different command signals, $U_{command}$, U_{LL}, U_{reflex}, and ffb were compared, and as expected, the feedforward force command was the primary indicator of behavior. Analogous to the proposed feedforward position command, pre-filter feedforward force commands were estimated as square pulses. At longer disturbance durations, when artifacts were not such prominent features of the dynamic data, the proposed square force pulses and the algorithm used to fit them were quite competent at achieving 'good' fits.

4.4.2 Force feedback

The contribution of the force feed*back* signal, while significantly smaller, was found to be nonzero in these tasks. Perhaps other disturbance rejection experiments in which subjects employ force control mechanisms that are not so predictable as the ones which allow for sufficient feedforward compensation, would rely on a larger contributions from force feedback.

4.5 Conclusions and future work

To summarize, experimental results from two subjects rejecting disturbance forces and concurrently making reaching movements were likely consistent with explicit time based force control. The proposed model generally estimated anatomically plausible parameters and accounted for the dynamics

by introducing feedforward and feedback force control commands. However, cerebellar compensation methods were not explicitly excluded as explanation for the observed abilities. We were able to neither confirm nor deny the existence of a minimum pulse duration, or the hypothesis that longer forces are created from a summation of shorter *subforces*.

With relative simplicity one might be able to make the desired conclusions upon resolving the probable equipment issue, as a feasible model has been tested, and analytical methods derived. Also, the work done here made the simplifying decision that analysis would be done assuming a single degree-of-freedom system. A logical continuation would be for the model to be converted to two joints. Also, one could attempt to model the observed behavior using simulations both with and without explicit force control to see if cerebellar error based control would be sufficient or whether explicit force control is in fact necessary to explain the data.

Chapter 5

Appendix

Appendix: Subject's Instructions For Experimental Tasks

5.1   Setup

- use *only* arm muscles, keep the rest of your body still

- be as relaxed as possible, especially your arm muscles, even for disturbance rejection

- sit up straight, feet flat on the floor in front of you

- your left arm may rest on the table or in your lap

- the wristguard is worn to assure that the only two joints moving are the shoulder and elbow, NOT the wrist

- the upper arm band hanging from the ceiling is to rest your arm, all tasks must be done in the horizontal plane

- sit so that during the farthest point in the task the arm is not fully outstretched

- the computer screen will be approximately 80cm in front of you to the left
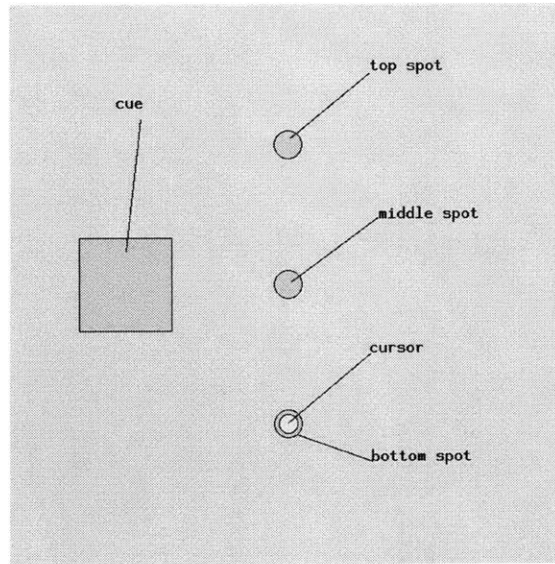
Figure 5-1: Experiment Display

5.2 Schedule

	BLOCK NUMBER	DISTURBANCE DURATION	TRAINING TRIALS	TESTING TRIALS
movement	1	n/a	40	20
isometric force rejection	2	250ms	60	40
moving force rejection	3	250ms	60	40
isometric force rejection	4	200ms	60	40
moving force rejection	5	200ms	60	40
isometric force rejection	6	150ms	60	40
moving force rejection	7	150ms	60	40
isometric force rejection	8	125ms	60	40
moving force rejection	9	125ms	60	40
isometric force rejection	10	100ms	60	40
moving force rejection	11	100ms	60	40
isometric force rejection	12	75ms	60	40
moving force rejection	13	75ms	60	40
isometric force rejection	14	50ms	60	40
moving force rejection	15	50ms	60	40

- testing will occur at least 2 hours after training

- training session lasts about 2 hours

- test session lasts about 1.5 hours

5.3 Tasks

5.3.1 Movement task

- begin by putting cursor inside bottom circle (see Fig. 5-1)

- after 1.5 seconds tracker spot will move from the bottom spot to the top stop (ignore the black spot)

- the goal is to move at about the same speed as the tracker, following the same straight trajectory

- another goal is for this movement to become almost a reflex, something that you don't need to think about but just happens when the tracking spot appears

- the movement is 20cm and it will take 3 seconds to move from start to finish

5.3.2 Force rejection tasks

- for the first five trials of isometric force rejection and moving force rejection do not try to reject the disturbance, just be floppy and get a feeling for the disturbance strength and duration

- after the first 20 trials of the isometric force rejection and moving force rejection tasks there, will be random 'catch trials': trials in which the force is cued as normal, but never comes on, this is a test for me to see if you are using stiffness as the methodology for fighting the force field, or if a force in the negative x direction is being used (as it should)

- these tasks require extreme concentration, do not talk while the experiments are running, to pause during any of the trial blocks, just move the cursor away from the start point

Isometric force rejection task

- begin by putting cursor inside the middle circle (see Fig. 5-1)

- after 1.5 seconds the cue will start blinking, this cue informs when the disturbance will begin and how long it will last, according to the color and blinking time (ignore the black spots), ie for a 250ms disturbance the cue will do the following:

BLUE	GRAY	BLUE	GRAY	BLUE	GRAY	RED
250ms	250ms	250ms	250ms	250ms	250ms	250ms

- the goal is for the cursor to remain in the same spot, ie using as little energy as possible (no cocontration = no stiffness) do an equal and opposite force pulse, the force pulse looks like Fig. 5-2.
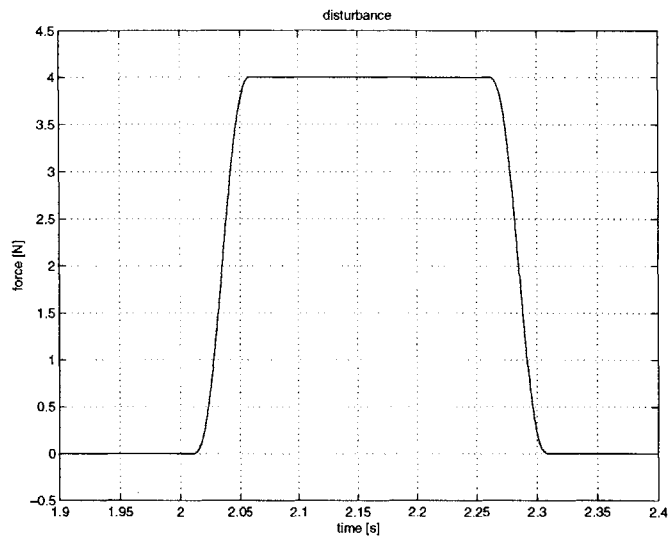
Figure 5-2: Disturbance

Moving force rejection task

- this trial is a combination of the movement task and the isometric force rejection task

- begin by putting the cursor inside bottom circle (see Fig. 5-1)

- after 1.5 seconds the tracker will begin moving from the bottom to the top spot, at a random time during the movement the cuing will begin for the force rejection following the same scheme as before (blinking three times then turning red)

- the goal is to continue making the straight movement but to add another, separate task to reject the disturbance, the disturbance will happen at a random time so that the two tasks are not merged

- again, the goal is to use as little effort as possible to move and reject the disturbance

5.4   Hints for force rejection

- count 1...2...3...4 with the blinking light to get disturbance onset and duration right

- when the force is rejected properly it will feel weaker

- the data I am looking at is position *and* forces recorded on the manipulandum handle, even if it does not look like there is much movement due to the disturbance, especially for faster forces, you still need to make an effort to reject the disturbance

- if initially pushed to the right, it means you are coming on too late with your force (or are not pushing hard enough), if initially pushed to the left, then pushing too early or too hard (usually its the timing and not the strength that causes movement)

- making the movement exactly in the tracker not critical, what is is to keep moving in a smooth motion that takes three seconds to get from start to finish

Bibliography

[1] James Ashe. Force and the motor cortex. *Behavioral Brain Research*, 87:255–269, 1997.

[2] Michael A Conditt, Francesca Gandolfo, and Ferdinando A Mussa-Ivaldi. The motor system does not learn the dynamics of the arm by rote memorization of past experience. *Journal of Neurophysiology*, 78:554–560, 1997.

[3] Michael A Conditt and Ferdinando A Mussa-Ivaldi. Central representation of time during motor learning. *Proceedings of the National Academy of Sciences*, 96:11625–11630, September 1999.

[4] Joseph A Doeringer and Neville Hogan. Intermittency in preplanned elbow movements persists in the absence of visual feedback. *Journal of Neurophysiology*, 80:1787–1799, 1998.

[5] DJ Bennett et al. Time-varying stiffness of human elbow joint during cyclic voluntary movement. *Experimental Brain Research*, 88:433–442, 1992.

[6] Tamar Flash and Neville Hogan. The coordination of arm movements: an experimentally confirmed mathematical model. *Journal of Neuroscience*, 5:1688–1703, July 1985.

[7] H-J Freund and HJ Budingen. The relationship between speed and amplitude of the fastest voluntary contractions of human arm muscles. *Experimental Brain Research*, 31:1–12, 1978.

[8] Hiroaki Gomi and Mitsuo Kawato. Human arm stiffness and equilibrium-point trajectory during multi-joint movement. *Biological Cybernetics*, 76:163–171, 1997.

[9] Z Hasan. A model of spindle afferent response to muscle stretch. *Journal of Neurophysiology*, 49:989–1006, 1983.

[10] Richard B Ivry. Force and timing components of the motor program. *Journal of Motor Behavior*, 18:449–474, 1986.

[11] JG Keating and WT Thach. No clock signal in the discharge of neurons in the deep cerebellar nuclei. *Journal of Neurophysiology*, 77:2232–2234, April 1997.

[12] F Lacquaniti, F Licata, and JF Soechting. The mechanical behavior of human forearm response in transient perturbations. *Biological Cybernetics*, 44:35–46, 1982.

[13] Steve G Massaquoi. *Modeling the function of the cerebellum in scheduled linear servo control of simple horizontal planar arm movements.* PhD thesis, MIT, 1999.

[14] T E Milner. A model for the generation of movements requiring endpoint precision. *Neuroscience*, 49:487–496, 1991.

[15] Reza Shadmehr and Ferdinando A Mussa-Ivaldi. Adaptive representation of dynamics during learning of a motor task. *Journal of Neuroscience*, 14:3208–3224, May 1994.

[16] Mandayam A Srinivasan and Jyh shing Chen. Human performance in controlling normal forces of contact with rigid objects. *Advances in Robotics, Mechatronics, and Haptic Interfaces*, 49:119–125, 1993.

[17] AAM Tax, JJ Denier van der Gon, CCAM Gielen, and M Kleyne. Differences in central control of m. biceps brachii in movement tasks and force tasks. *Experimental Brain Research*, 79:138–142, 1990.

[18] Kurt A Thoroughman and Reza Shadmehr. Learning of actions through adaptive combination of motor primitives. *Letters to Nature*, 407:742–747, 2000.

[19] Michel Treisman, Andrew Faulkner, and Peter LN Naish. On the relation between time perception and the timing of motor action: evidence for a temporal oscillator controlling the timing of movement. *Quarterly Journal of Experimental Psychology*, 45A:235–263, 1992.

[20] Rolf Ulrich and Alan M Wing. A recruitment theory of force-time relations in the production of brief force pulses: the parallel force unit model. *Psychological Review*, 98:268–294, 1991.